AERO 402

Cislunar Navigation & Communication Constellation

CDR Document

Matthew Trotter

Eric Comstock | George Colts-Tegg | Can Zhang

Victoria Torres | Daniel Kirby | Kevin Ott

Texas A&M University
Department of Aerospace Engineering

Spring 2022

Table of Contents

I. Executive Summary

Main Science Goal

The primary goal is to support development of lunar infrastructure through providing high data rate communications and high precision navigation services. Reducing the cost, risk, and unknowns for future moon missions will encourage further missions.

Mission Requirements

- The system shall be capable of returning up to 100GB/day of science data to Earth as well as providing high-quality audio and video with a maximum of ten simultaneous users in cislunar space and on Earth.
- The system shall supply users with location data that is accurate to within 0.5 meters on the lunar surface.
- The system shall supply users with location data that is accurate to within a radial distance of 20 meters in orbit.
- The system shall operate for three years.

Mission Concept and Instrumentation

The mission will consist of 20 identical satellites each with a mass of 70.54 kg, volume of 0.0595 m^3, and 3 antennas that will support Earth communication, customer communication, and navigation. Earth and customer communications will be handled using a parabolic antenna operating in Ka band, and navigation will utilize a patch antenna in S band. An ensemble of sun sensors and inertial sensors are used for attitude determination while 3 reaction wheels are used for attitude control. An onboard computer, two software-defined-radios, and an amplifier are used to directly support communication and navigation. To support the communication scheme a data rate of 9.3 Mb/s has been established; therefore, providing ample data transmission for GNSS support and scientific data transmission. 4 chip-size atomic clocks are used for accurate timekeeping for navigation. Power will be generated using Multi-junction solar cells spanning 0.84 m^2 which will generate approximately 430 W at the beginning of life in a sun-facing environment. Power will be stored in a single battery with an energy capacity of 512 Wh allowing for surplus energy to be stored. A 10N Bi-propellant thruster alongside fuel tanks for N_2O_4 and Monomethylhydrazine will provide sufficient propulsion for all orbital maneuvers. For the proposed 3 year mission, the delta V required for Atlas V insertion error, orbital parameter targeting, station keeping, and hyperbolic departure sums to 657.43 m/s with the departure accounting for approximately half.

Orbit and Constellation Design

The satellites are evenly distributed over 5 planes evenly spread in RAAN and phased evenly within each plane. The frozen orbits selected have a semi-major axis of 8025 km, an inclination of 39.5°, an eccentricity of 0.004, and an argument of periapsis of 270°.

CONOPS

- The constellation leaves Earth's surface on a lunar insertion burn on the Atlas V launch vehicle.
- The constellation will deploy in Lunar orbit, releasing all stowed instrumentation.
- After appropriately correcting burns, the constellation will support the primary mission objectives.
- Once the constellation reaches its prescribed end of life each satellite will initiate a hyperbolic transfer to achieve a heliocentric graveyard orbit to prevent any damages to ongoing lunar surface exploration or development.

II. Introduction

Background and Motivation

Networked communications on Earth have revolutionized the way we live. The ability to simply and reliably contact anyone we want to at our own leisure is something that has become second nature to us as humans. This has introduced new ways to not only communicate with our loved ones but also has made collaboration between one another that much easier. Because of how vital network communications are to us here on earth, it is easy to deduce that as we look to colonize the lunar surface, Mars and beyond, we will want the ability to communicate there just as we do on Earth. Because of this NASA (National Aeronautics and Space Administration has begun to research ways of going about implementing such infrastructure. One of the proposed solutions to this engineering challenge is NASA's very own LunaNet.

Currently, space agencies around the world are focused on studying the Moon and developing semi-permanent infrastructure. A few of the major planned missions are the International Lunar Research Station [11] planned by Roscosmos and the China National Space Administration as well as NASA's very own Artemis Plan [12]. These are just the two largest, multi-year projects which will need support both in orbit and on the Lunar surface in the coming years. In order for these missions and others like them to be successful there must be infrastructure in place that provides high speed communication and accurate navigation for anywhere on and around the moon. To do this, there would need to be a constellation around the moon that employs the same methodology of tracking position as the United States' GPS (Global Positioning System) system. The main criteria for this is that there will be four satellites in view of any given location of the lunar surface. Once this infrastructure is in place it will improve the probability of success of these Lunar missions as well as reduce costs, and as a result future missions to the Lunar surface will be encouraged.

High Level Mission Requirements

ID	Description	Rationale	Traceability	Verification Strategy
0.01	The system shall be capable of streaming high definition audio (96 kHz sample rate) and video (720p) for up to 10 simultaneous users in cislunar space and with Earth.	Crews for the return missions to the moon will be approximately 2 - 4 passengers each. Therefore there is not a need to supply communication services for more than 10 users at any given time.	Stakeholder Need	Multi-Access Validation, IV.6.8.
0.02	The system shall allow for position determination on the lunar surface with a resolution of 0.5 m.	Required for the ability to accurately give crew directions based on their location on the lunar surface.	Stakeholder Need	Position Error Validation, IV.6.1. Use the procedure described in "Understanding GPS/GNSS: Principles and Applications" by Elliott Kaplan and Christopher Hegarty [9]
0.03	The system shall allow for position determination in orbit around the moon with a resolution of 0.5 m to an altitude of 500m.	Required for the crew in orbit to accurately make course corrections based upon their given location.	Stakeholder Need	Position Error Validation, IV.6.1. Use the procedure described in "Understanding GPS/GNSS: Principles and Applications" by Elliott Kaplan and Christopher Hegarty [9]
0.04	The system shall be capable of a data throughput of 100GB/day	Required based upon the amount of science that is expected to be conducted.	Stakeholder Need	Link budget calculation, IV.6.3
0.05	The system shall remain operable for 3 years.	Required to justify the cost of the mission.	Stakeholder Need	System Lifetime Validation, IV.6.6. Identification of system components with the shortest lifetimes and analysis of expected nominal operation.

0.06	The TT&C subsystem shall have a minimum BER of 10^-5.	Required for timely and accurate communication for both customers and the system itself.	0.01, 0.04	Link budget calculation, IV.6.3
0.07	The system shall have an average dilution of precision of 6 or less over at least 90% of the moon.	Necessary for end users of the GNSS system, and comes from the analysis of ephemeris data error and time error. This coverage assures that key scientific sites can have high precision.	0.02, 0.03	Orbit STK Simulations and Analytical Equations, IV.6.2
0.08	The system shall have a maximum latency of 5000 ms between the Earth and the Moon.	Required for timely and accurate communication for both customers and the system itself.	0.01	Link budget calculation, IV.6.3
0.09	The system shall have communication availability of at least 95%.	Required for timely and accurate communication for both customers and the system itself.	0.04	Orbit STK Simulations, IV.6.2
0.1	The system shall be capable of a data throughput of 2 Mbps per customer.	Required to achieve the quality of audio and video streaming required.	0.01	Link budget calculation, IV.6.3

III. Concept of Operations

Historically, the Atlas V successfully launched and carried payload into lunar orbit in 2009 [16]. Due to the flight heritage and other considerations, such as fairing size, the Atlas V is selected to carry the CNCC system to a designated parking orbit around the Moon. After arriving at the parking orbit, the CNCC satellites released from Atlas V transfer to their operational orbits. During operation, the CNCC allows fast, easy-to-access communication between objects on or near the Moon and with ground stations on Earth. The ADCS system allows for the accurate pointing that enables communication between the Moon and Earth. The CNCC is equipped with a propulsion system that allows for necessary orbital maneuvers to be executed and for general station-keeping while in Lunar orbit. At the end of its lifetime, the hypergolic thrusters onboard send CNCC into a heliocentric graveyard orbit.

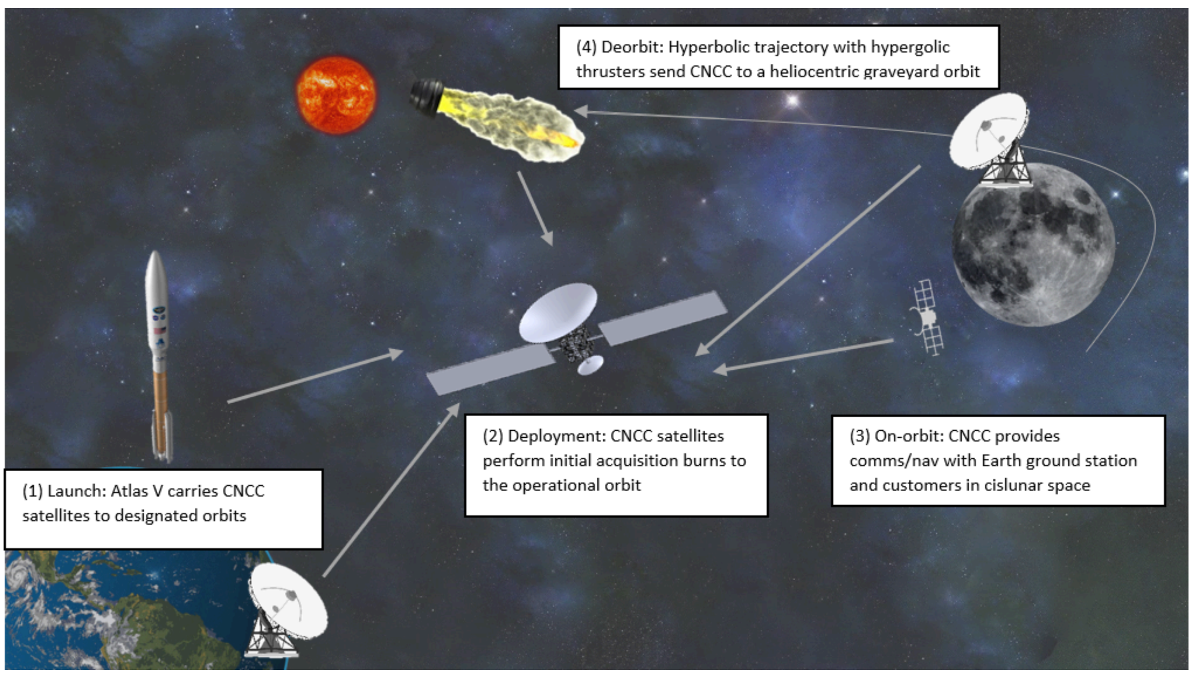

Figure 1. Diagram of CONOPs overview

The next few subsections will explain the concepts of operation during each mission phase in detail.

Launch Strategy (T+0)

The launch vehicle chosen is Atlas V designed by Lockheed Martin, which has the mass capacity of up to 2652 kg to the Moon. Before loading, the solar panels and parabolic antennas are folded to minimize the occupied volume, with a similar mechanism to Queqiao satellite launched in 2018. Then, all CNCC satellites will be placed and secured in the fairing of Atlas V waiting for launch.

After the launch, the CNCC satellites will be carried inside the Atlas V along a designed trajectory to the translunar region, just like the LRO and LCROSS satellites previously. Approaching the vicinity of lunar parking orbit, the lunar orbit insertion sequence starts to prepare for the deployment of CNCC satellites.

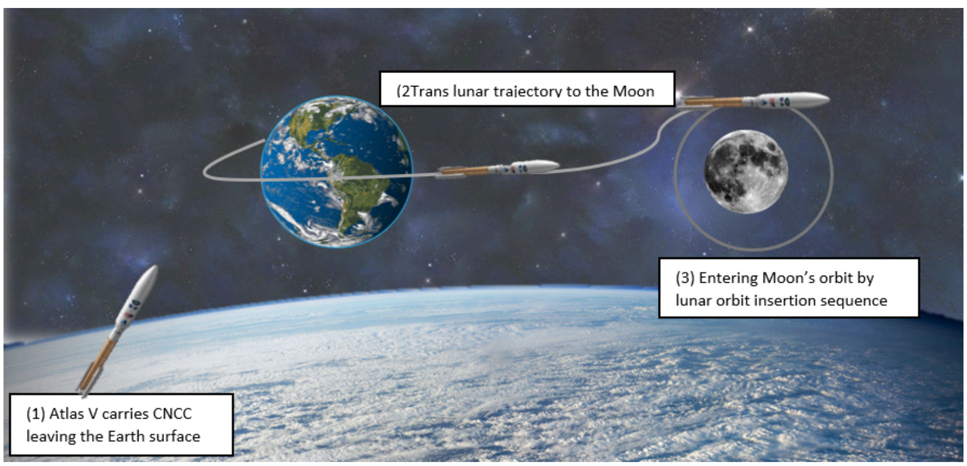

Figure 2. Diagram of launch strategy

Deployment Strategy (T+5 Days)

During the achieved trans-lunar trajectory the spacecraft will be switched off inside its deployer and a power connection with the Atlas V will keep the CNCC constellation batteries charged. Once the Atlas V reaches the vicinity of the moon, the Canisterized Satellite Dispenser (CSD) is released, and the actuators on the CSD release the lids holding down the satellites, and a spring pushes the satellites out. After de-tumbling and deployment of the solar arrays and parabolic antennas, the payload and all sub-systems will be commissioned. The onboard ADCS will activate initial acquisition mode to obtain rough altitude information, and telemetry will begin with Earth for more precise orbit determination. After stabilizing the satellite, the full satellite control will use a propulsion system to aim for final operational orbit. The satellite will cruise with radiometric navigation strategy and Direct-To-Earth communication and perform station keeping and wheel desaturation maneuvers.

The nominal mission phase begins with the attainment of the mission orbit and continues for 3 years. During this phase routine operations, non-routine operations, and data communication and processing will be performed.

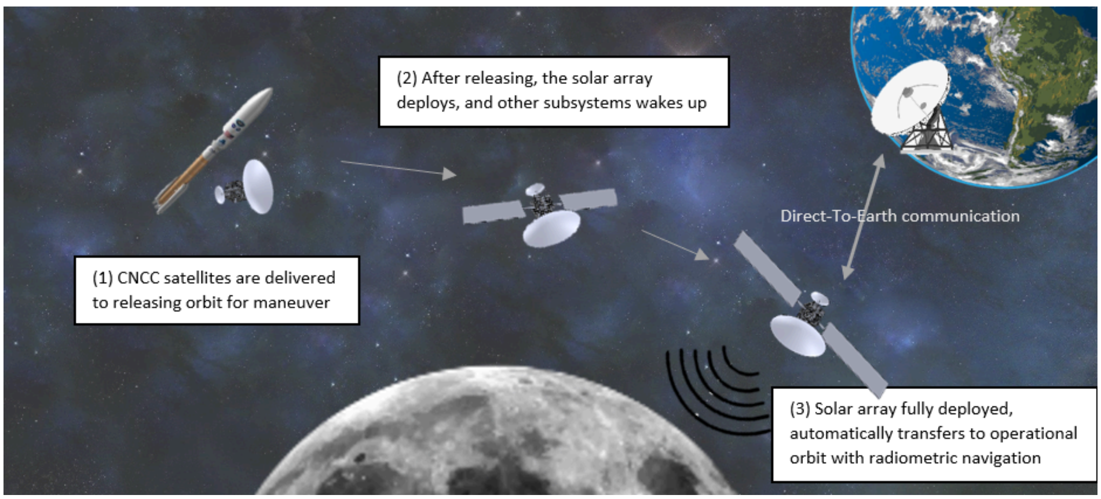

Figure 3. Diagram of deployment strategy

On-orbit (T+7 Days)

While the CNCC satellites are on their operational orbits, a few major instruments would engage to achieve the high-level communication requirements.

The entire satellite will be governed by an onboard computer that serves as a control center. All data will be gathered and processed here, and all commands are sent by this primary computer. In order to synchronize trajectory data with other satellites and ground stations, the atomic clock and ephemeris are updated periodically from the ground station. This step is crucial for accurate position determination of the CNCC. To achieve multiple communication schemes, antennae, Software Defined Radios (abbreviated as SDRs), and power amplifiers integrate to enhance the signal quality. Two of the antennas on each satellite transmit and receive signals from customer or ground stations, while the third navigation antenna constantly transmits a navigation signal. The SDR processes the received signals and generates signals on the proper frequency with correct modulation and encoding. To increase the output of SDR, a power amplifier is utilized. The selection of the instruments will be emphasized in Section IV.

With the three antennas onboard that serve for various types of communication, several critical communication schemes are specified --

- Direct communication, with Lagrange relay, or the mix of two
- Nearside and farside of the Moon
- Multiple coverage for sparsely and densely spaced
- Multiple-Input and Multiple-Output (MIMO)

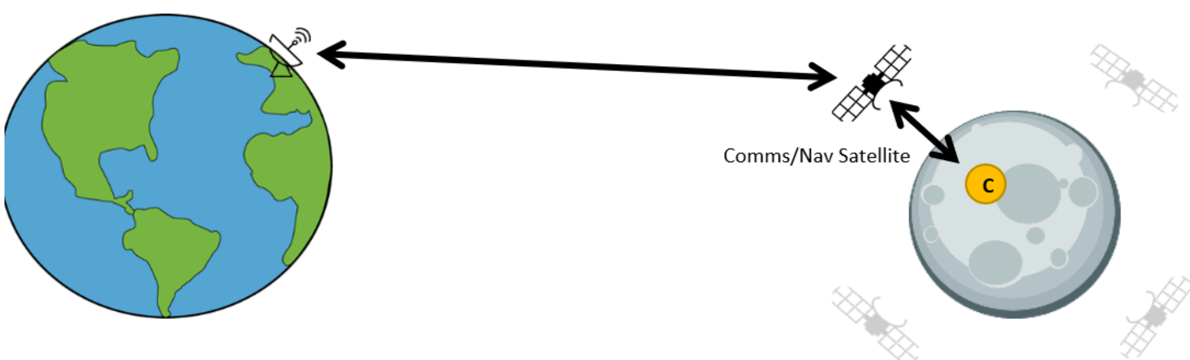

Figure 4: Communication Scheme 1

Communication scheme 1 is the typical and generic scenario where a satellite can directly speak to a customer and to Earth simultaneously with no additional connections.

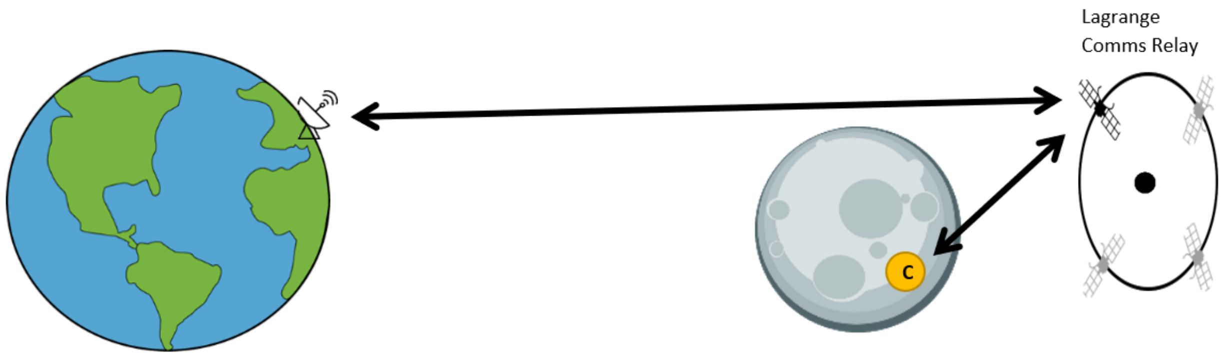

Figure 5: Communication Scheme 2

Communication scheme 2 represents the communication scheme where a satellite speaks directly to a Lagrange relay satellite. A single Lagrange relay satellite with a very large antenna could potentially improve the performance of the entire constellation by improving the efficiency of Moon to Earth communication.

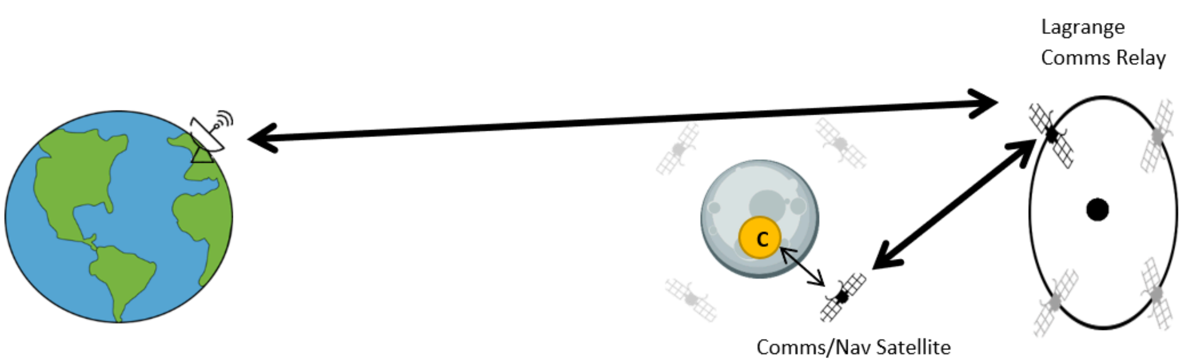

Figure 6: Communication Scheme 3

Communication scheme 3 demonstrates a scenario where the system discussed in this paper supports communication with a Lagrange relay, drastically reducing the required power from the customer and greatly enhancing the data throughput of the system. Because the satellites are designed such that they could all talk to Earth independently, it is without a doubt they could use a Lagrange relay with little trouble and greatly improve their ability to satisfy the high-level requirements laid out. However, the design complexity of the entire CNCC system will increase significantly with the Lagrange relay. Thus, we decided to adapt the communication scheme 1 for scope of this project and showed the high-level requirements could still be fulfilled in later sections. In the further study, communication scheme 3 will be taken into consideration.

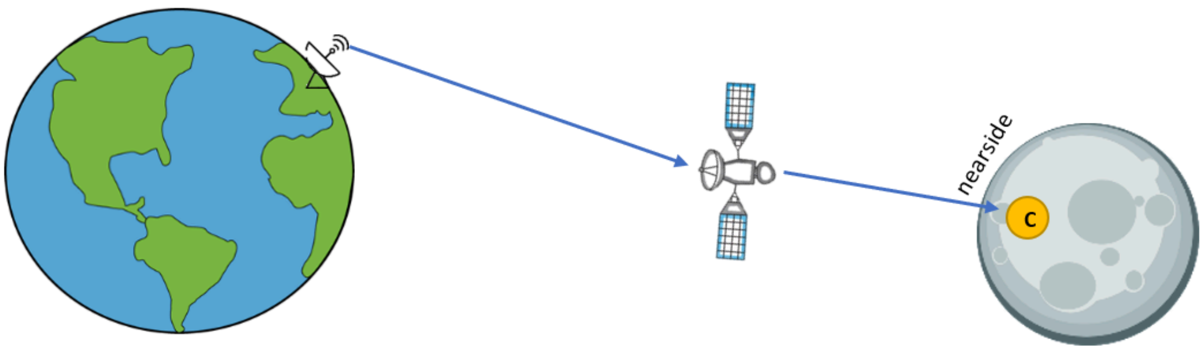

Figure 7: Communication Scheme 4

Communication scheme 4 is virtually identical to communication scheme 1 but is meant to highlight the difference between communication scheme 1 and communication scheme 5, where a satellite in sight of a customer does not have sight of Earth. In this situation, only a single relay satellite is needed and latency is minimized. The Earth communication antennae is body-fixed, so the satellite is oriented toward the Earth. The solar panels and customer antenna have independent gimbals/actuators so they can be pointed independently, maximizing the sunlight absorbed and the power received/transmitted to the customer.

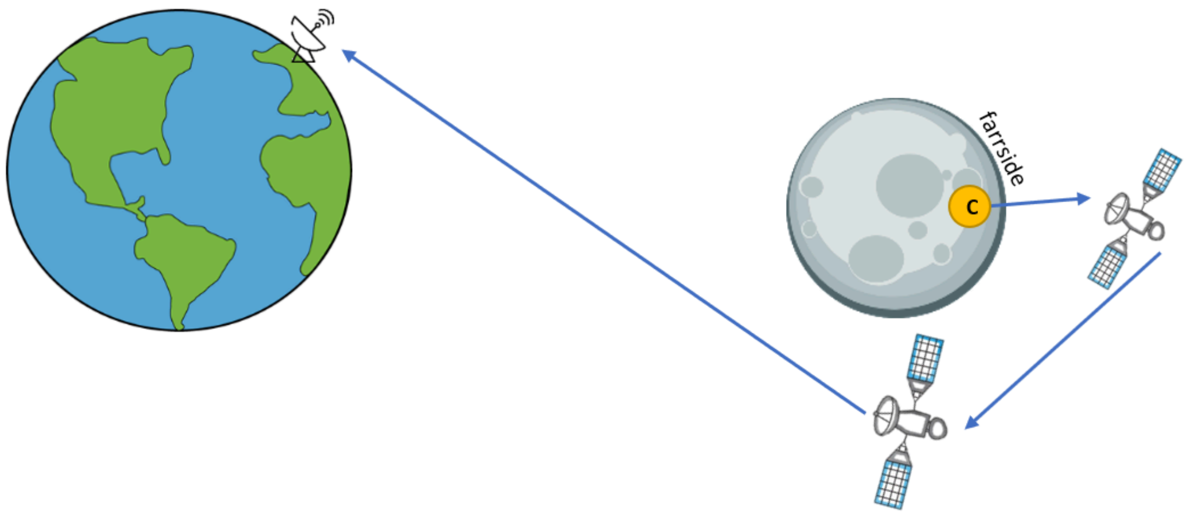

Figure 8: Communication Scheme 5

In Communication Scheme 5, the customer communicates with a relay satellite that has no view of a ground station. In this scenario, the body-fixed Earth communication antenna is instead used to communicate to the customer antenna of another relay satellite. This orients the first relay satellite, the one in communication with the customer, toward the second relay satellite. The satellite knows how to aim at another relay satellite because the ephemeris data that is periodically updated for the navigation system contains the ephemeris data for every satellite in the constellation. Therefore, with some straightforward calculations, the first relay should be able to determine if another relay satellite in the constellation is in view, and if that relay has sight (or, at least, should have sight) of a ground station. This will allow for a chain of communication to take place that will allow for rapid communication with Earth. Although this scheme does introduce more latency inherently (more relays means more latency), it is necessary for any communication to take place at all.

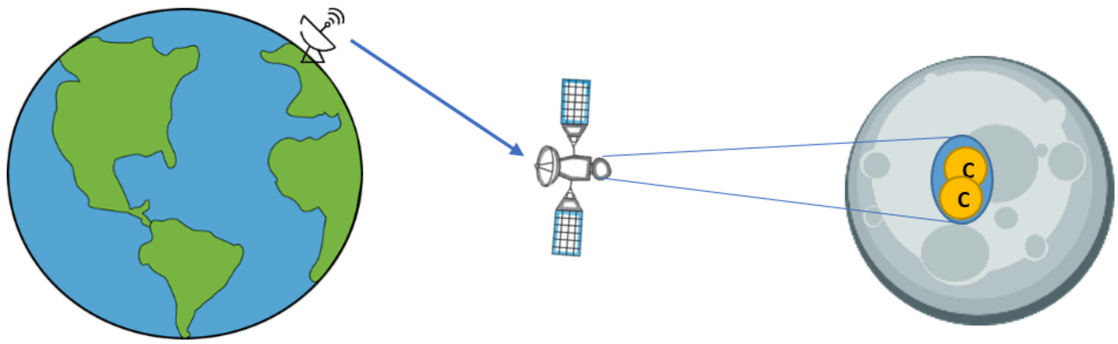

Figure 9: Communication Scheme 6

Communication scheme 6 demonstrates the first way that multiple customers could be serviced by a single satellite. As long as the customers lie within the half-power beam width of the customer antenna (which constitutes a 9657 km^2 area), simply transmitting and receiving with a single satellite can be easily done. To allow multiple connections to a single satellite network effectively, a Time Division Multiple Access (TDMA) technique is implemented. A precise time synchronization is required to achieve TDMA, which is satisfied with the onboard atomic clocks used for navigation. TDMA is considered advantageous over other multi-access schemes because it reduces total noise at any time (the antenna is not receiving multiple signals simultaneously from sources with potentially very different transmitting powers), does not require a particular encoding scheme (making it more accessible by a variety of systems), and these two factor combined should mean that a TDMA system should have a lower cost and mass for the customer. This is very contextual to this constellation though. Because synchronization is so incredibly important, TDMA is usually disadvantageous in comparison with CDMA. Because this constellation is filled with atomic clocks constantly being resynchronized and a navigation signal being constantly transmitted with time information, this constellation comes equipped with the means to make TDMA preferable. Another major disadvantage of TDMA that usually makes it less preferred than CDMA is the reduced data throughput due to guard times. This is not so critical because this communication scheme should be used very rarely, Communication Scheme 7 is the preferential multi-access scheme for this constellation. This is used only in the event that more than 4 customers are in a location that is only in view of 4 satellites. According to the requirements, we must support 2 Mb/s for each of the 10 customers we are required to support. Because the total data throughput of 4 CNCC satellites is approximately 37.2 Mb/s, only about 54% of the total data throughput is required. This means the required frame time and guard times will not hinder our meeting of the requirements.

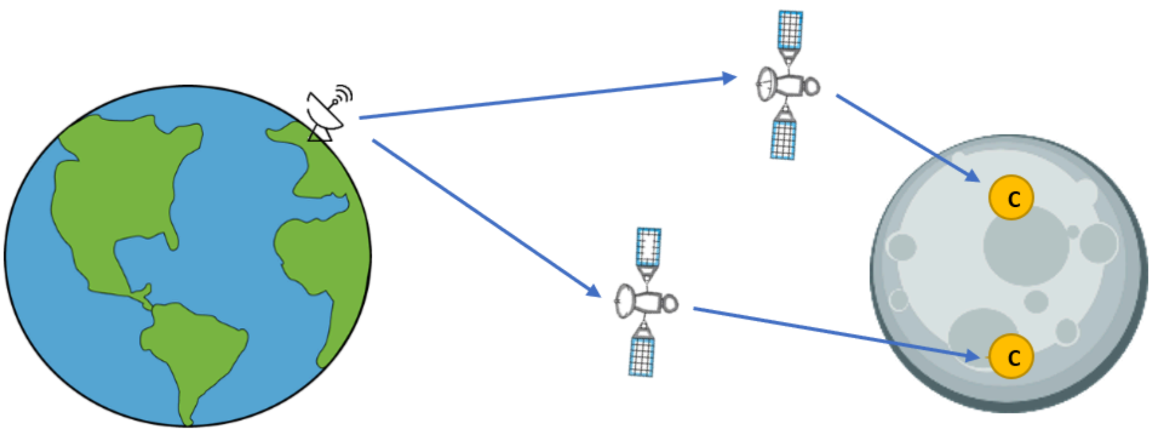

Figure 10: Communication Scheme 7

Communication scheme 7 demonstrates the second way that multiple customers could be serviced. This scheme involves multiple satellites, which is required in situations where customers do not sit within the same half-beam width of a single satellite. As there are multiple antennas in view of every location on the moon at all times, we demonstrate that we can easily service up to and beyond 10 customers simultaneously.

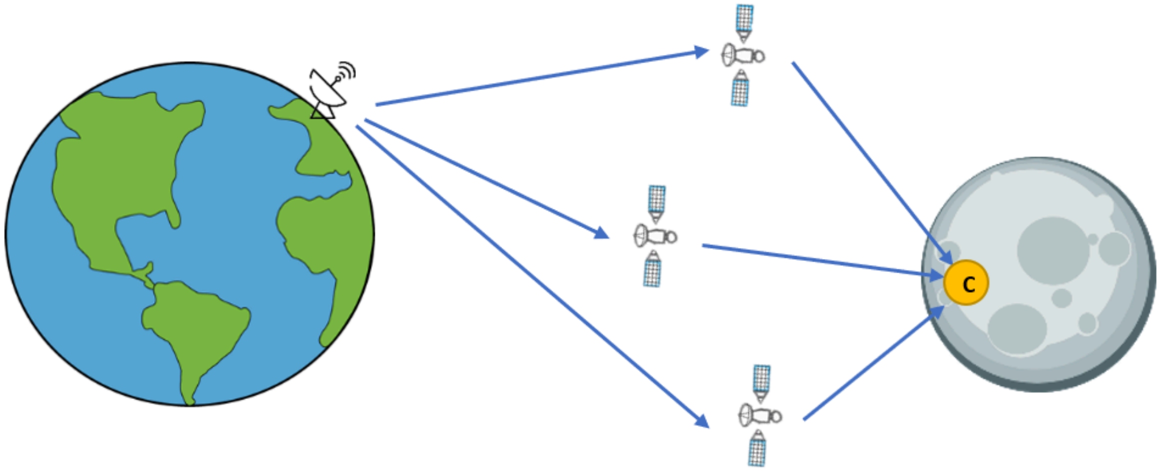

Figure 11: Communication Scheme 8

Communication scheme 8 demonstrates a scheme where MIMO communication is employed to greatly enhance the bit error rate and the data throughput for a single customer or multiple customers in the same half-power beam width. This has been demonstrated previously in many simulations and in a space mission [17][18][19]. The space mission has validated the simulation results which demonstrates that data throughput could be increased by up to 4 times in 2x2 MIMO schemes. This means that we could facilitate missions and customers that may need more data throughput than what our constellation is initially designed for, demonstrating the adaptability of the constellation.

Deorbiting Strategy (T+3 Years)

The primary deorbiting strategy is to initiate a hyperbolic departure with gravity assist from the Moon to heliocentric orbit. One advantage of deorbiting to a heliocentric graveyard orbit is that the period is long compared to the period of common space mission orbits. Thus, even if there is a chance of conjunction with spacecraft, it is extremely rare on a time scale of centuries.

However, the hyperbolic departure is not always necessary. Per IADC-02-01 Space Debris Mitigation Guidelines, artificial spacecraft at its terminating operation phase could re-entry as one of the deorbiting strategies to guarantee not interfering with other spacecraft and reduce the residual orbital life. Therefore, if an unforeseen event happens to one of the satellites, a controlled crash landing into the Moon will be planned to avoid collision with other artificial objects [20].

The hyperbolic departure is preferred though due to the stated science goals of the CNCC. By supporting the building of infrastructure on and around the moon and encouraging more moon missions, it is imperative to not disrupt these missions that are being encouraged by creating even a small chance that one of the satellites in the constellation could collide with any of the newly created lunar infrastructure.

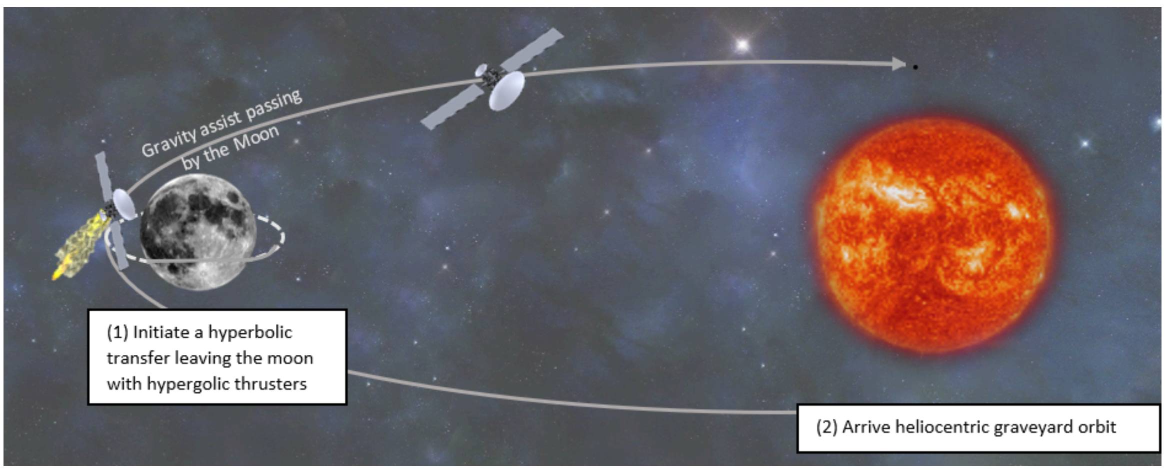

Figure 12. Diagram of deorbiting strategy

IV. Baseline Design

The mission concept consists of 20 identical satellites each equipped with key instrumentation that supports both communication and navigation.

Communication is supported by a body-fixed Earth communication parabolic antenna with a 1.1 meter diameter operating on Ka-band which is pointed with the spacecraft's attitude control system. Another articulable customer communication parabolic antenna with a diameter of 0.37 meters is used to communicate with customers at certain locations on the moon. Articulation is supported by a gimbal, and accurate pointing is achieved with an ensemble of sun sensors, inertial sensors, and a star tracker.

Navigation is supported by a 0.1 x 0.1 m patch antenna array in the S-band mounted to the face of the CubeSat structure which transmits the required GNSS signal. Accurate time is maintained by an ensemble of 4 on-board chip-sized atomic clocks. The communication system will be used to periodically update ephemeris data and time data. The ephemeris almanac will be stored and updated as appropriate with the onboard computer.

Customers will be able to determine their position by using multiple of the constantly transmitted navigation signals. Communication can be supported in a multitude of ways as discussed in the CONOPS and is proven in the instrument selection and design section.

Section 1. Instrument Selection and Design

Our key instrumentation is constituted by the antennae, SDRs, power amplifiers, and power instrumentation necessary to support the links within our communication network. To optimize our entire communication scheme, we used a DOE and a genetic algorithm.

The link budgets were performed for the following three schemes: CNCC to Earth, CNCC to Customer, and Customer to CNCC. The DOE and optimization are focused on minimizing both the mass and power of the key instrumentation and the necessary supporting equipment.

The design space is as follows: only parabolic antennae will be considered with diameters ranging from 0.1 m to 4.0 m. Only the S, X, and Ka bands will be considered. Every link budget will be allowed to have its own band.

The evaluation of each scheme considers losses unique to each band (especially atmospheric losses unique to Ka), different ground stations characteristics for each of the bands in the Near Space Network, whether or not a power amplifier is necessary (This is the case if the SDR can't output the proper amount of power for the required signal strength), the required solar panel and battery masses necessary to support the power found in the link budget, the sum of all link budgets, and the different SDRs required for each band.

Using a Latin Hypercube Sampling scheme, the DOE was formed and the following Pareto frontier was found:

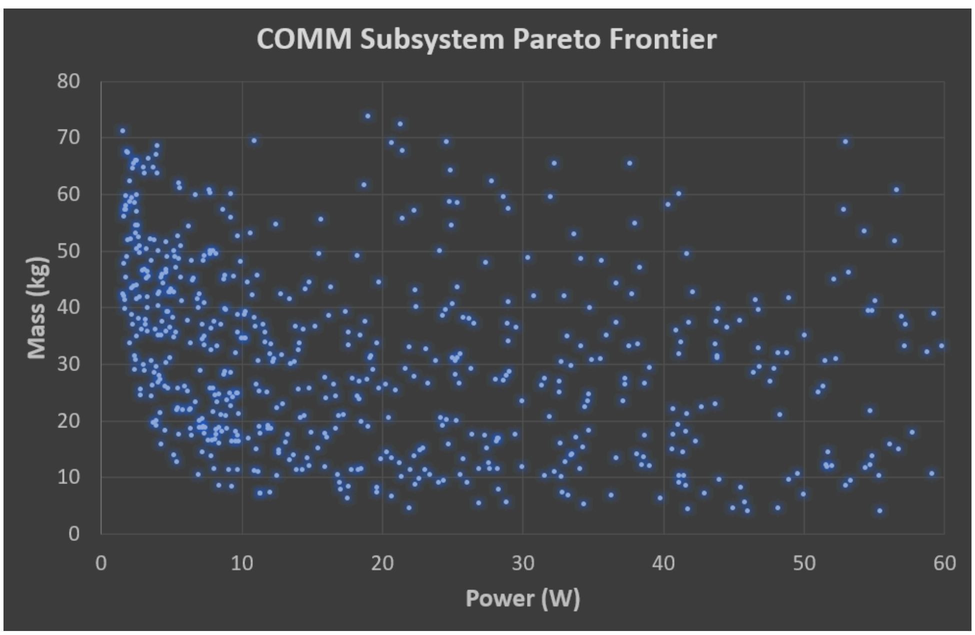

Figure 13. Pareto front of mass and power of different key instrumentation configurations

Using the designs that lay on the Pareto front oriented toward our utopia point of (0,0), we can create the first generation of our genetic algorithm.

The genetic algorithm created had the following attributes: the population size was maintained at 5. The top 2 designs of any generation were kept. Crossover was performed at random (50/50 chance of a child pulling an attribute from either of the parents for each attribute) and the mutation rate was set at 5%. For the discrete variables, the number that the algorithm handles remained a float, while when evaluating the system architecture the float was rounded to the nearest integer. The fitness function was the reciprocal of the sum of mass and power times 1000 (This is simply done so that the fitness function was not a small number prone to round-off errors). The number of generations varied until a plateau was observed.

The following graph shows the fitness of the system improving over the generations and the corresponding plateau in fitness:

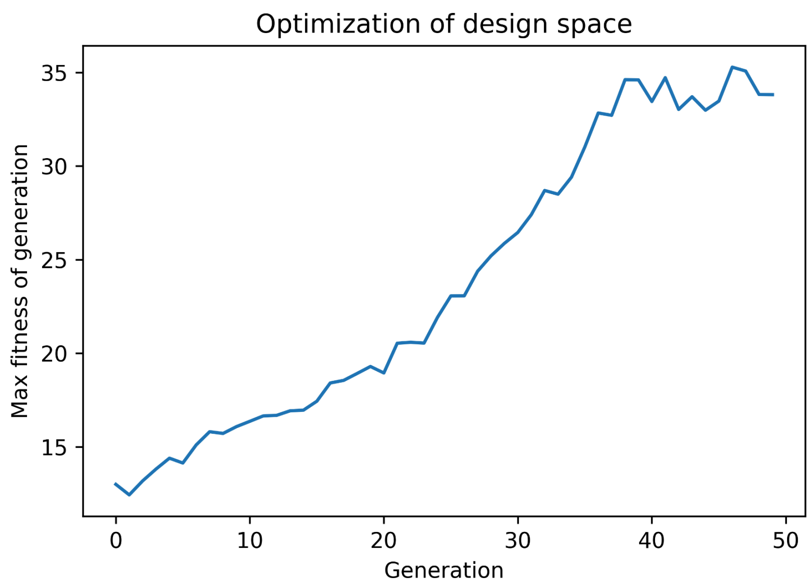

Figure 14. Best fitness of each generation from the genetic algorithm.

Selecting the best design from the final generation, we obtain the following system: a 1.1 m diameter Ka-band (26 GHz) Earth communication antenna and a 0.37 m diameter Ka-band (26 GHz) Customer communication antenna. From the architecture evaluator used, this system is expected to consume 21.9 W and have a total mass of 4.61 kg. The link budget details are as follows:

Link Budget	Earth - CNCC Comm	Customer - CNCC Comm
Frequency	26 GHz	26 GHz
Eb/N0	10.5 dB	10.5 dB
BER	10^-8	10^-8
Line loss	1 dB	1 dB
Transmitter gain	46.9 dB	37.5 dB
Receiver gain	71.6 dB	40.1 dB
Data rate	69.7 dB	69.7 dB
Noise temperature	28.3 dB	21.3 dB
Transmitter pointing loss	0.083 dB	0.083 dB
Receiver pointing loss	0.083 dB	0.083 dB
Space loss	232.4 dB	198.6 dB
Rain attenuation	8.98 dB	0 dB
Margin	3 dB	3 dB
Modulation	BPSK	BPSK
Bandwidth	50 MHz	50 MHz
Channel Encoding	LDPC	CCSDS-TC/M

Table 1. Link budget details of the optimized communication architecture.

The channel encoding was simply chosen based on the encoding required for the NSN and the capabilities of the selected SDR (Blue Canyon). Space loss was determined by the maximum distance from the Earth to the Moon for the Earth communication link budget, and for the customer communication link budget the ’maximum minimum distance’ was used (the maximum expected distance between a customer and a satellite based on STK simulations). This will be discussed further in the orbit and constellation design section.

Another key piece of instrumentation was the navigation antenna. Because our preliminary analysis was showing that this part of the design was not as intensive, the selection of the navigation antenna was more prescriptive than for the communication antennae.

For the navigation analysis, we assume that the customer has a 40x40 mm patch antenna in the S-band (based on a cursory search for S-band patch antennae). The assumed rate of data transfer was 50 bits per second, which is similar to the GPS system. Using the ’maximum minimum distance’ again (meaning the received signal should actually typically be much better), we can perform our link budget also with the Blue Canyon SDR. A patch antenna array of size 0.1 m x 0.1 m with a mere 3 W of power was enough to support the link budget and have a received power of greater than -150 dB which is the more typical measure of quality for received GNSS signals. The details of the link budget are below:

Link Budget	Navigation
Frequency	2 GHz
Eb/N0	10.5 dB
BER	10^-8
Line loss	1 dB
Transmitter gain	4.87 dB
Receiver gain	-3.08 dB
Data rate	17 dB
Noise temperature	21.3 dB
Space loss	176.4 dB
Margin	3 dB
Modulation	BPSK
Bandwidth	50 MHz
Channel Encoding	CCSDS-TC/M

Table 2: Link budget details of the link budget for navigation.

This analysis may be slightly inaccurate, as the channel encoding scheme may not be allowed to be CCSDS-TC/M. The GPS signal on Earth is a semi-encrypted signal due to national security concerns. This team was not able to find any documentation/ regulations specifying that a cislunar navigation system would also require this type of encryption, but an actual introduction of this plan may spur action from legislators that would require it. This is a hole in the analysis that can be rectified by simply increasing the power to compensate for the loss due to encryption.

Section 2. Orbit and Constellation Design

Constellation		
Total Satellites, 20	Plane(s), 5	Satellites per plane, 4

Orbital Elements		
Inclination, 39.5°	Argument of periapsis, 270°	RAAN, $p_i \cdot 72°$ where $p_i = 0, 1, 2, 3, 4$
Eccentricity, 0.004	Semi-major Axis, 8025km	Phase, $s_i \cdot 90°$ where $s_i = 0, 1, 2, 3$

Table 3. Orbit and Constellation Details

As shown in Table 2, the constellation consists of five orbital planes evenly spaced over the right ascension of the ascending node. Each plane consists of four satellites evenly phased over the plane. With an argument of periapsis of 270°, a semi-major axis of 8025 km, inclination 39.5°, and eccentricity 0.004, our satellites sit within a frozen orbit around the moon. Due to our mass and budget limitations, it was key that this team selected orbits with a minimum amount of station keeping and required the minimum amount of satellites to satisfy our DOP requirements.

This semester, this team built an architecture evaluator for constellation designs that allowed us to automatically generate constellation designs that could be completely variable. The use of the simulator had to be limited though due to how long the simulations took. In the interest of increasing the amount of constellations that could be analyzed, the simulator was first configured to perform low resolution scans (3x3 latitude and longitude points evenly spaced, every 10 minutes over an orbit period), select the best architectures from the low resolution scans, and then perform high resolution scans (15x15 latitude and longitude points evenly spaced, every 10 minutes over a sidereal month). The recursive and iterative process performed throughout the duration of this project actually made the orbit design unfortunately prescriptive.

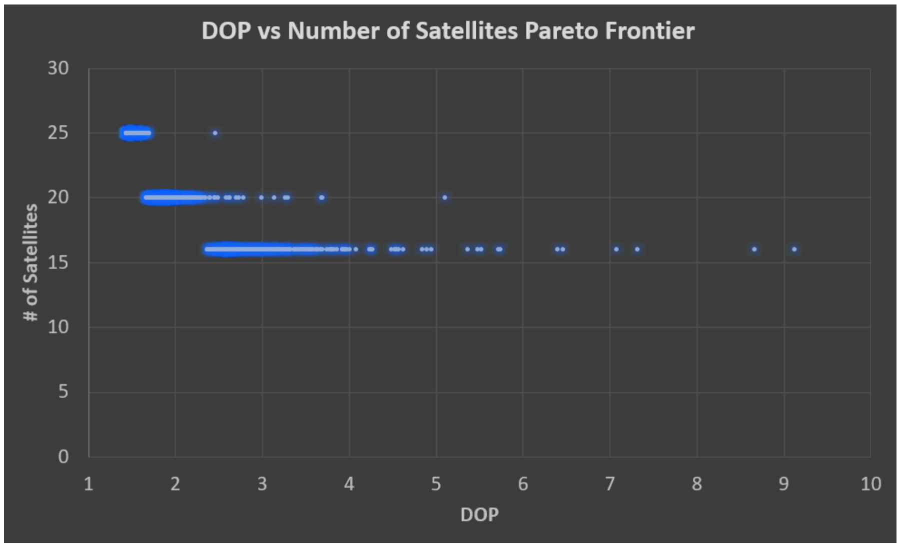

Figure 15: DOP vs Number of Satellites, a Pareto Frontier

This Pareto frontier demonstrates two things: first, that a greater number of satellites correlates with a lower DOP, and second that as the number of satellites increases, designs become less sensitive to the particular details of the constellation design, allowing more freedom. Therefore, this immediately makes the goal of the team reducing the per unit cost of each satellite as much as possible so the greatest number of satellites could be used within the budget. This motivated the team to build satellites as small as possible and use COTS components as often as possible. The team was successful in using COTS components for every single part of the satellite except the parabolic antennae and the navigation patch array antenna. Making the satellite small was another matter; mission requirements drove selection of instrumentation that necessitated a 27U cubesat chassis. After our initial economic analysis, it was realized that only 20 satellites were going to be possible for this mission within the budget constraints. From the above pareto front, it is clear that we are more sensitive to our orbital parameters.

A key part of reducing the per unit cost was minimizing the required stationkeeping of orbits. More stationkeeping requires more propellant, better thrusters, and larger tanks. It also intrinsically drives up the chance of failure of the mission, more firing of the thrusters means a greater chance that a thrust could fail. From the analysis of the 1500 orbits, the following relationship was found between a value proportional to the delta-V required for stationkeeping and semi-major axis:

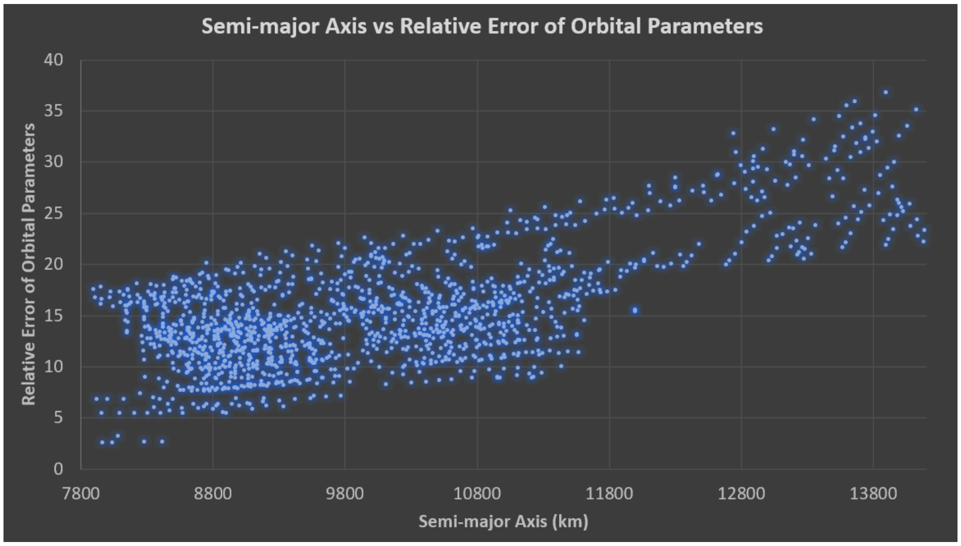

Figure 16: Semi-major axis vs. Relative Error of Orbital Parameters

The simulator was not prescriptive with the stationkeeping scheme. Instead, orbits were allowed to simply drift for the period for which they were analyzed. To compare orbits against one another without having to simulate a variety of stationkeeping strategies, we used a 'relative error of orbital parameters' calculation. This is simply the relative error of each orbital parameter in a root-mean-square error calculation. This is not perfect, as the stationkeeping required to account for the relative error in each orbital parameter is NOT equal. But a metric was needed to compare orbits, and clear and expected relationships began to arise. While DOP improved as the altitude of the constellation was increased, the stationkeeping cost and the maximum minimum distance increased such that the tradeoff was not favorable. Making the altitude as small as possible was also not possible, as the DOP began to decrease radically with only 20 satellites. Therefore, this team was locked around 8,000 km to maximize DOP, minimize the 'maximum minimum distance', and minimize stationkeeping (for 20 satellites). This motivated the team to go ahead and select a frozen orbit configuration, and led to the selection of the frozen orbit discussed above.

The calculated dilution of precision for this orbit, using the simulator which was validated against the Pereira 2019 [5] paper, showed a DOP of 4.73 and the DOP was beneath 6 over 93% of the lunar surface. This satisfies our system level requirements which supports the high-level mission requirement of determining position to 0.5 m. The method for calculating DOP is discussed in IV.6.2.

This orbit was also desirable because the maximum minimum distance (the largest distance between any satellite and a point of interest at any point at any time) was only 7,841 km. With an average minimum distance of 6,577 km, we can easily satisfy our link budget requirement without requiring a large burden on the customer for communication. It also helped reduce the required power for transmission of the navigation signal. By easing the requirements for all of these link budgets, we more easily satisfy our high-level requirements for communication.

Section 3. Spacecraft Design

The overall spacecraft, as has been described thus far, requires the following mass and power budgets:

Dry Mass	Mass (kg)	Margin (kg)	Mass+Margin (kg)
Battery	3.2	0.32	3.52
LO-Determination	0.055	0.0055	0.0605
Thrusters	2.6	0.26	2.86
Heaters	3.96	0.396	4.356
Computer	2.2	0.22	2.42
Atomic Clock	0.336	0.0336	0.3696
ADCS Sensors	3.8	0.38	4.18
Reaction Wheel	8.8	0.88	9.68
SDR	0.39	0.039	0.429
Antenna Pointing Assembly	4.4	0.44	4.84
Solar Array pointer	1.16	0.116	1.276
Radiator	4	0.4	4.4
Power Amplifier	2.637	0.2637	2.9007
Anetnnae Mass	3.174	0.3174	3.4914
Fuel Tank Mass	2.404	0.2404	2.6444
Solar Array	1.9	0.185	2.0
10% Margin			4.9
Totals	**45.0**	**4.3**	**54.4**

Table 4. Mass budget per satellite

	Power Consumption (W)				
	Max Com/Nav Mode	Typical Com/Nav Mode	Orbit Eclipse Mode	Lunar Eclipse Mode	Maneuver Mode
Battery	30.0	44.9	-	-	-
LO-Determination	2	2	2	2	2
Thrusters	0	0	0	0	9.6
Heaters	0	0	0	30	30
Computer	12.2	12.2	12.2	12.2	12.2
Atomic Clock	20	20	20	0	0
ADCS	1.8	1.7794	1.8	0	3.9
SDR	5.4	5.4	5.4	0	0
Actuator Pointing	0.01270	0.0127	0.01270	0	0
Solar Array pointer	0.0114	0.0114	0	0	0
Power Amplifier	50.1	50.1	50.1	0	0
Earth/Com Antenna	17.48	4.37	17.48	0	0
Customer/Com Antenna	2.3	0.575	2.3	0	0
Nav Antenna	3	3	3	0	0
Safety Margin 30%	43.29105615	43.29555	34.28763353	13.26	17.29836
Total	187.6	187.6	148.6	44.2	57.7

Table 5. Power budget per satellite

The components of the spacecraft are as follows:

Subsystem	Quantity per satellite	Instrument Selection
ADCS	1 2 2 4 N/A	Inertial navigator STIM300 Star sensor ST-400 Tensor Tech FSS100 Reaction wheel NRWA-T2 Thruster (Same as in propulsion)
Power	1 30 1	VES16 8s4p battery module Triple Junction UTJ solar panels NanoAvionics EPS Maximum Power Point Tracking (MPPT) power conditioning and distribution unit
Propulsion	1 2 2 2 1	10N Bi-propellant thruster Rolling diaphragm tank Pyro valves Fill and Drain Valves Pressure Regulator

C&DH	1	3U CompactPCI single-board computer
Thermal	8	Microvascular Carbon Fiber Channel Radiator
TT&C	1 1 3 2 1 4 2	Parabolic antenna 1.1 m Parabolic antenna 0.37 m Patch antenna 0.1 x 0.1 m Blue Canyon SDR Moog Type 33 Gimbal MAC-SA5X (Atomic clock) RF-Lambda RFLNPA4547A Power Amplifier

Table 6. Instrument List

Our instrumentation selection was guided by our requirements. Our primary concerns are ensuring our ability to point quickly and accurately, the ability to provide thrust for insertion burns, station keeping, and hypergolic departure, our ability to transmit at our selected frequency with enough power and with the correct modulation, our ability to properly generate and store power, and our need to properly keep time onboard the spacecraft for navigation purposes.

Another key piece of instrumentation that needs to be discussed is the SDR.

Figure 17. Picture of the Blue Canyon SDR

For our communications, it is key that we have the hardware needed to support transmitting and receiving in frequencies of interest (Ka- and L-band), modulating and demodulating in BPSK, supporting our data rate of 9.3 Mb/s, and it needs to fit into the CubeSat 27U chassis. The Blue Canyon has all of this functionality and can even support data rates up to 15 Mb/s, but can only transmit with a power of 1.25W. For this end, we need to also connect the SDR to a power amplifier. This team has found a power amplifier taking the 1.25W output signal and can increase its output all the way to 200W, which exceeds our needs. This SDR also has incredibly small dimensions, not exceeding 5 mm in any dimension. Thus, it can clearly fit in our chassis. The Blue Canyon SDR is able to support the channel encoding schemes discussed in Section 1, which correspond to the NASA Near Space Network requirements.

Section 4. Ground Segment Selection

Our selected station is the Near Space Network operated by NASA. This ground station supports multiple Ka-band antennas with 18.3 diameter parabolic antennas. By operating at the Ka-band, the amount of power and the required size of our antenna to achieve our desired data rates with our desired bit error rate become reasonable. The gain of these ground antennas is also sufficient to support our 1.1 meter Earth communication antenna.
Recent developments in small satellite technology has allowed for the use of Ka-band antennas as a part of the Near Space Network by CubeSats and other small satellites [2].

The following table explains the capabilities and parameters of the Ka antennas the Near Space Network supports:

Characteristic	Value
Frequency	25.5 – 27 GHz
G/T	46.98 dB/K, 10° elevation, clear sky
Polarization	RHC or LHC
Antenna Beamwidth	0.04 deg
Antenna Gain	70.5 dBi
Demodulation	BPSK, QPSK, OQPSK, (SQPSK), AQPSK, UQPSK, (AUQPSK, AUSQPSK, AUSQPSK
Data Rate	235 Mbps single decoder mode 470 Mbps dual decoder (I&Q)
Data Format	NRZ-L, M, S, DNRZ
Decoding	CCSDS Compliant Viterbi Convolutional Decoding

Table 7. Cited from reference 1.

The following table details the rain attenuation that has been recorded when communicating with the antennas in this network:

Ground Station	Elevation Angle	Rain Attenuation (dB)			
		90% Availability	95% Availability	99% Availability	99.9% Availability
WS1 (White Sands)	5°	1.84	3.08	8.98	40.15
	10°	1.07	1.82	5.47	28.94

Table 8. Cited from reference 1.

The cost of the network depends very much on the mission at hand. NASA recommends using a rough estimate of $557 per 30 minutes for S, X, and Ka-band [3]. This system operates fundamentally as a relay for users on the moon, so the full burden of this cost does not fall squarely on this team or their budget. A portion of the cost would be expected to be handled by the users of the CNCC. The Near Earth Network (NEN) was chosen over the Deep Space Network (DSP) due to the expected congestion. Many missions wish to utilize the DSP, but this saturation could lead to bottlenecks in overall data transmission. Failure to maintain the required data rates due to supporting infrastructure was deemed unnecessarily risky, and therefore the NEN appeared most optimal. From the requirements, 100GB/day is expected to be transmitted. For the duration of the 3 year mission it is expected to result in approximately 110TB of data. Assuming the satellites can transmit at a rate of 10Mbps with the ground station and the NEN cost estimation rates hold, then an estimated cost of $9,758,640 is expected for transmission. This cost can be supported by the budget given for the mission.

Section 5. Launch Strategy

The selected launch vehicle is the Atlas V. In comparison to other launch vehicles, the Atlas V is more reliable, affordable, and has an appropriate fairing to fit our satellites. Deployment of the constellation will involve only one launch, with all 20 satellites being deployed. The satellites will be deployed into one of the operating orbits, with all appropriate satellites performing burns to shift their right ascension of the ascending node as necessary. Then, all satellites will perform required phasing burns as needed in each plane.

The stowed configuration of the satellite was estimated by approximating the volume taken up by the solar cells (Which have a length of 1.93 m and a width of .43 m, with an approximated thickness of 2 cm) and folding that volume such that it conformed tightly to the sides of the satellite, as is done with many other small satellites. The patch antenna already is tightly to the side of the satellite. The two parabolic antennas were estimated by assuming their footprint took up a whole face of the satellite, and that the remaining length was folded up to make a cylinder (similar to the scheme used for the Queqiao satellite). This means the 1.0 m parabolic antenna constitutes a cylinder with a radius of .05 m and a height of 0.44 m. This allows us to approximately evaluate if the stowed configuration of the satellite could sit within the Atlas V fairing.

The following image shows how all 20 of our satellites, with their antennas and solar panels in a stowed configuration, fit within the medium version of the Atlas V launch vehicle payload fairing:

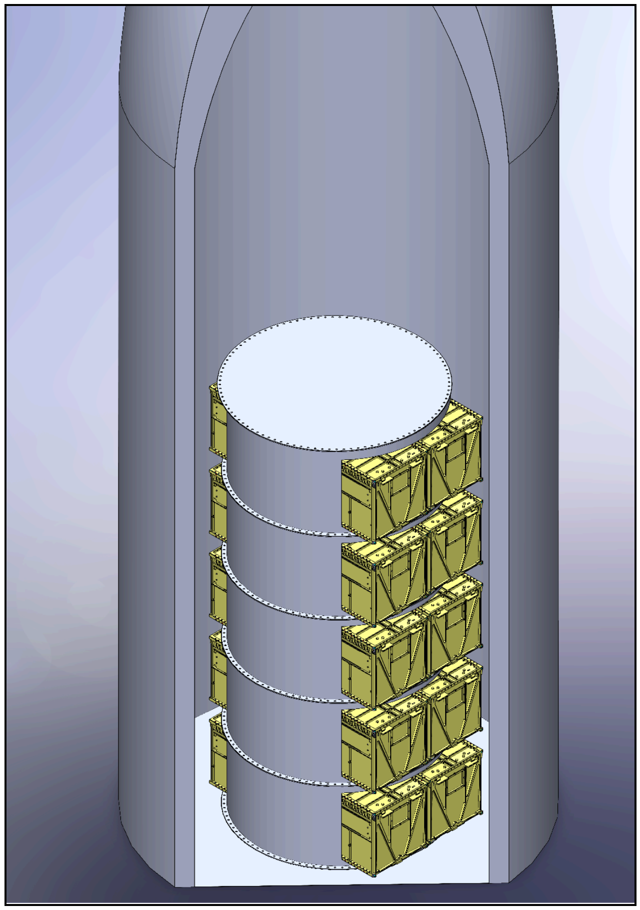

Figure 18. CAD of a simple satellite model within the Atlas V fairing

The satellites will be deployed using a Canisterized Satellite Dispenser (CSD) designed for 27U cubesats. Given that 27U cubesat schemes are at a TRL level of 4, commercially available CSDs for this specific application do not currently exist; however, there are no engineering or technological extenuating constraints for the development of this size CSD. Therefore, to approximate the cost and weight of this deployment scheme, extrapolation of current commercially available options for 3U, 6U, and 12U cubesats CSD's will be the basis for cost and weight estimations. Using a linear approximation from commercially available CSD, an estimated weight of 9.5kg is achieved. The CSDs will mount to a secondary flight adapter similar to the CubeStack design from LoadPath. Using data from Loadpath it can be estimated that the weight for a 27U variant would be 53.2 kg. For our deployment scheme 5 of the cubestack 27U variants will be used resulting in a total weight of 266 kg. Combining both CSD and the cubestack, will significantly reduce the risk of damage to the payload as both have proven methods of force damping.

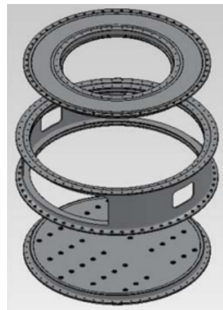

Figure 19. Cubestack secondary payload adapter

Section 6. Validation

6.1 Position Error Validation

The position error of our system determines the reliability of our navigational capabilities, and as such is an extremely important figure of merit. As we need to support lunar operations, a low position error is essential. According to requirements 0.02 and 0.03, a position error at or below 0.5 m is required for successful operation. Thus, an analysis of our system to validate its satisfaction of this requirement was done. From Moore, the position error can be determined by adding the sources of error (Alan variance and frequency drift.) at the time directly before a resynchronization, and then multiplying by the DOP and the speed of light to determine the maximum position error, as shown in the following equation.

$$E_x = \sqrt{\frac{E_{t,Alan}(t_{sunc})^2 + E_{t,F.D.}(t_{sync})^2}{N_{clocks}}} \cdot DOP \cdot c$$

As the maximum position error was already determined, this validation mainly focused on the required clock resynchronization times to achieve this level of accuracy. Clock resynchronization periods were found to be the deciding factor since as they synchronize both the frequency and the time on the clocks with those on Earth, they would reset both the major sources of error considered in the analysis, thus resetting position error to zero. While other factors such as DOP, clock accuracy rates, and the number of clocks (as the multiple clocks on each satellite could be synchronized with each other, reducing error), were considered, these factors affected many other subsystems, and so clock resynchronization period was considered as the variable, with the other parameters as constants. Thus, we could determine whether our system was able to function on a realistic clock resynchronization period - a system requiring clock resynchronization every millisecond to maintain accuracy would be impossible to use.

The first of these error sources was the Alan variance - caused by errors in measurement, or deviations from the expected results due to the unpredictability of quantum effects. The Alan variance is typically expressed as a frequency drift, but due to its predominantly random nature, its intensity declines with the square root of the time elapsed in accordance with the law of large numbers. The intensity of this effect on different timescales was given on the datasheet of the atomic clock being used [10].

The other major effect we considered is frequency drift - which, while less intense in short timescales (less than a few minutes, in the case of the atomic clock chosen for our system), this phenomenon gets worse over time. This is because it is composed of errors in the system that manifest as *permanent* shifts in frequency (at least until the clock can be recalibrated). Although the *rate* of frequency drift climbs with the square root of the time elapsed - again, in accordance with the law of large numbers - the actual amount of frequency drift increases with the square root of time elapsed. This makes it a huge problem at large timescales. The intensity of this effect on different timescales was also given on the datasheet of the atomic clock being used [10].

The errors mentioned above were calculated, added in accordance with error propagation methods, and the resulting time error was multiplied by the speed of light and by the average DOP factor found by the simulation. The resulting calculation, while accurate in the case of a single atomic clock being used, did not accurately model the fact that multiple atomic clocks were being used on each satellite so they could correct each other, and that the satellites were also constantly relaying data. Approximately 80 atomic clocks would be in lunar space communicating at any given time, so the resulting answer was divided by the square root of 80 to account for this. A table of the quantities found, and the equations used to derive them, is given below.

Reset time (between synchronizations)	1020	s	Input: This value was used as a control variable.
# Clocks considered	80		Input: 4 clocks were used for 20 satellites to give 80 total.
Alan Variance	1.58E-12		Proportional to the square root of the reset time; proportionality constant derived from data on [10].
Frequency Drift	2.40E-12		Proportional to the cube of the square root of the reset time; proportionality constant derived from data on [10].
Time drift	0.00000000292924819 7	s	Determined by taking the square root of the square of the Alan variance added to the square of the time drift, and multiplying by the reset time.
Speed of Light	299792458	m/s	Physical Constant
DOP	4.73		Input: Determined using STK simulation's average DOP in next section.
Position error (maximum time error)	0.46	m	Output: Determined as time drift multiplied by DOP and speed of

			light. This is the position error right before resynchronization, at its maximum effect.
Position error (average)	0.23	m	Output: Average position error over interval between resynchronizations.

Table 9. Summary of quantities used to derive position error

These formulas were then made dependent on the time between resynchronizations as an input. Through experimentation, it was determined that a resynchronization time of 17 minutes provided a position error of 0.46 m. Notably, the error would only be this large right before a resynchronization, so the average error would be about half of this, 0.23 m. Regarding the resynchronization time, 17 minutes is entirely feasible for a brief transmission of timestamps between a single satellite on the network (as this satellite will correct the times of the others), and will not represent a significant strain on our communications budget.

6.2 Orbit Validation

For orbit validation, it is important to calculate the dilution of precision such that we can estimate the position error for customers using the systems and thus validate requirements 0.02 and 0.03. DOP is calculated using the procedure described in reference [21].

We calculated using a grid size of 15x15 separated evenly over latitude and longitude over the course of one orbit, calculating DOP every 10 minutes.

To validate this strategy, we took Architecture 1 from reference [5] and plugged it into our simulator. Our simulator produced an average DOP of 4.73 while [5] calculated a DOP of 5.01. The discrepancy is explained by the difference in stratagems for calculating DOP (And possibly by limiting the number of satellites considered in the calculation, some analyses limit the number of satellites that can be considered in the DOP calculation).

Coverage is defined as DOP<6. With a 15x15 grid every 10 minutes over 1 orbit, you get ~1,000 DOPs over time and space. 93% of these DOPs were below 6. That is how coverage was calculated.

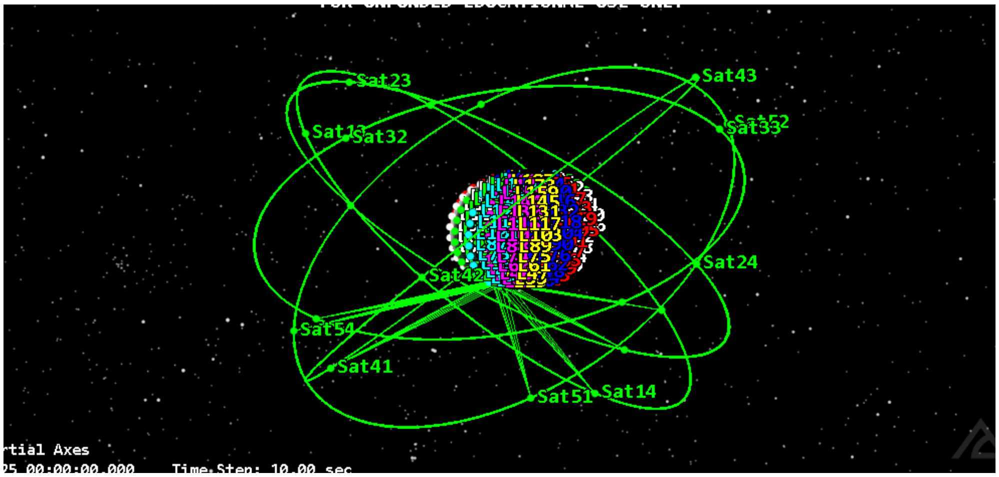

Figure 20. Image of the points created on the moon by a high resolution scan Line of sight and distance was recorded using STK.

6.3 Pointing Accuracy and Capability Validation

We will focus on the ADCS instrumentation as the other subsystems will be discussed at length in the baseline design section.

To satisfy our ADCS requirements, we need to be able to accurately evaluate our attitude and to be able to quickly modify it. Our half-power beam width for Earth communication is 0.243 degrees while our half-power beam width for customer communication is 0.483 degrees. As long as we can determine our attitude to within 1/12th of those half-power beam widths, we can easily satisfy the pointing loss in our link budget equations and thus satisfactorily communicate.

For our angular determination, we choose an ensemble of 2 Star Trackers (Berlin Space Technologies ST-400), 2 Sun Sensors (Tensor Tech FSS100) and 1 Inertial Measurement Unit (The STIM300), all of which are TRL 9 and consume a reasonable amount of power.

Sensor Tech FSS 100

Tensor Tech FSS 100

- Number of Units: 2
- Accuracy: 0.1 deg
- Total Power Usage: 0.0132W
- TRL: 9
- Total Mass: 0.008 kg

Figure 21. Picture of the FSS100 and its performance measures

STIM300

STIM300

- Number of Units: 1
- Accuracy: 0.3 deg/hr
- Power Usage: 1.5 W
- TRL: 9
- Mass: .055 kg

Figure 22. Picture of the STIM300 and its performance measures

ST400 Star Tracker

Berlin Space Technologies ST400

- Number of Units: 2
- Accuracy:
    - 5 arcsec in pitch & yaw
    - 40 arcsec in roll
- Total Power Usage: 1.34 W
- TRL: 9
- Total Mass: 0.70 kg

Figure 23. Picture of the ST400 star trackers and its performance measures

Due to the different characteristics of the sensors in the ensemble, different scenarios lead better or worse performance for the sensor depending on the specific characteristics of the scenario. For example, if the star sensor can see multiple stars, its accuracy is very high, but if no stars are in view the accuracy drops significantly. By using both sun sensors and star trackers, we balance the pros and cons of each sensor type. The accuracy in each scenario is as follows:

Control Mode	Conditions	Best Sensor Available	Accuracy	Average accuracy over a orbit (deg)	Comment
Acquisition	1) Requires attitude determination in short time, high-frequency sensors; 2) Eclipse period	1) Sun Sensors; 2) IMU	1) 0.1 deg; 2) 0.3 deg/hr	0.091736	Eclipse period can be avoided by carefully choosing releasing time
Orbit Insertion	1) Thruster firing (maybe unstable); 2) Eclipse period	1) Sun Sensors; 2) IMU	1) 0.1 deg; 2) 0.3 deg/hr	0.091736	Including both lunar orbit insertion and de-orbiting
Nominal/ Slew	1) Normal orbiting conditions 2) Slew	Star trackers	1) 5 arcsec for pitch & yaw; 2) 40 arcsec for roll	1) .00098209; 2) .0078567	Assume there are always stars in the field of view. The maximum slew rate of satellite will not affect star trackers
Contingency	1) Power outage; 2) Loss of stabilization; 3) SPEs or other intensive solar activities	1) Sun Sensors; 2) Sun Sensors; 3) IMU	1) 0.1 deg; 2) 0.1 deg; 3) 0.3 deg/hr	1) 0.070711; 2) 0.070711; 3) 0.30000 deg/hr	1) Sun sensors use the least power; 3) Although sensors chosen have high radiation tolerance, extreme solar activities can exceed their tolerance

Table 10. Summary of ADCS accuracy with different control modes

With these accuracy ranges, we find that the ratio between our half-power beam width to be 1/50th for Earth communication and 1/100th for customer communication, which is much less than 1/12th and thus easily satisfies our requirements for pointing and validates our link budget equations.

6.4 System Lifetime Validation

In this section we will analyze the spacecraft's battery, solar panels, and atomic clocks to determine the point at which they will become unusable for the mission, as well as several other components on the spacecraft that were found to be bottlenecks on our mission lifetime. In the following analysis, it was found that the most likely failure would likely be some form of instrumentation failure, after a time of roughly five years. However, the spacecraft's battery, clock, and solar panels were found to last much longer.

First, the atomic clock will be considered. Atomic clock frequency drift, discussed in section 6.1, can potentially build up to extremely high amounts if not corrected, which can lead to growing position errors that accelerate in magnitude (as the time deviation from frequency drift is proportional to the time elapsed to the power of 3/2). Our selection for an atomic clock mitigates this risk by including both digital and analog tuning devices capable of a range of 10^{-6} Hz/Hz [10], allowing it to accommodate the buildup of errors with updates from Earth. From the calculation used in section 6.1, it was found that the frequency drift only approaches 10% of the tuning range after an elapsed time of fifty-five thousand years - much longer than the other components of the mission will last, by far.

Also of concern is the system's battery. The battery we are currently using (the VES16 battery unit from Saft Solutions), is rated for 25000 cycles on its datasheet. As our orbital period is 61200 seconds (calculated from our orbital radius), and the battery is charged and discharged once per orbit, this gives us a lifetime for this component of 48.48 years, if the batteries maintain the same depth-of-discharge. As we can now show, this can be dramatically extended by gradually reducing the depth-of-discharge over time, which must be done anyway due to solar panel degradation.

Solar cell degradation can now be addressed. Assuming 3% geometric loss per year, the following time brackets can be derived from the fact that we produce 435.67 watts when operating at full capacity, we have an excess of 143.68 watts when in full sunlight, and we spend 130 watts, and 63.6 watts, respectively, on our navigational and communicational antennas. These numbers were taken from the spacecraft power modes found in section 3.

As we spend 4128.46 s in shadow for every 61200 s of mission (calculated from our orbital period and the diameter of the moon), we only need to produce 311.69 watts to continue operating at full capacity. We will drop below this power level after 10.99 years, and be forced to operate in a reduced capacity - going into lunar eclipse mode, which only draws less than one fifth the power, in the normal orbital eclipse periods.

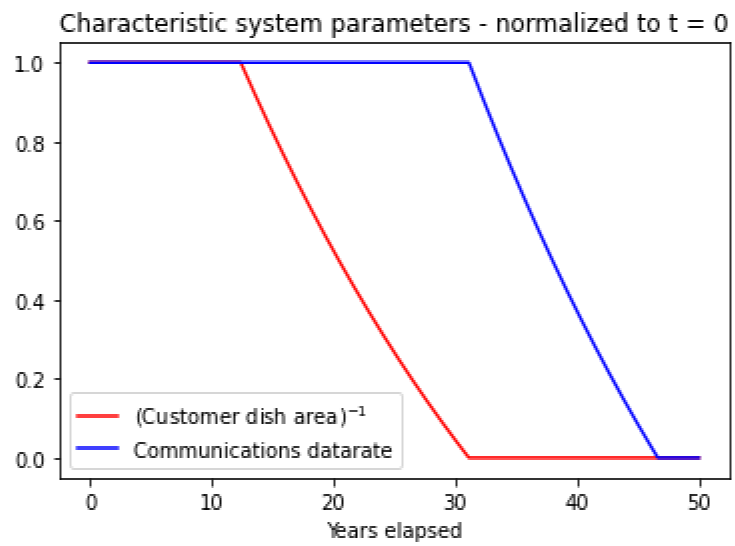

After 12.75 years, we will drop below 295.42 watts of power, and we will have to begin slowly cutting off navigational services to continue operating due to lack of power. While this will not directly impact our accuracy, we will nevertheless only be able to serve customers with larger antennas during this period, with required customer antenna size increasing asymptotically to infinity - shown in the figure to the right.

After 31.79 years, we will drop below 165.42 watts of power, and navigational services will be completely depowered. We will then have to start powering down communications as well, dropping data rate - shown in the figure to the right.

After 47.73 years, we will drop below 101.82 watts of power, and the spacecraft will no longer have the energy to maintain its original function. However, by going into a state similar to lunar eclipse mode permanently, we can maintain telemetry on the system, and potentially recover it for display and semi-functionality in a museum. This however depends on the political conditions of the time. Note that propulsion budgets do not have to be accounted for as well, for the final disposal of the satellite can be done without powering heaters.

After 70.53 years, we will drop below 50.83 watts of power, and further operation of the system in any capacity will become completely impossible, so we will be forced to dispose of the satellite using its propulsion system. It is expected that by this point the moon will be sufficiently terraformed that an atmospheric entry destroying the satellite will be possible.

However, though this analysis suggests a lifetime of decades, a further analysis of our satellite's components show that the ADCS star sensor has a five-year life expectancy, which effectively limits our mission to that timescale. Even if a workaround to this was found, the issue of delta-V for stationkeeping prevents our satellite from being able to last for more than seven years total, even if our hyperbolic departure fuel (amounting to 322 m/s of delta-V) was instead used for further stationkeeping (estimated to be 80.5 m/s per year). These values were pulled from section 6.9. In an optimistic scenario, this might be able to be increased to 8.05 years due to the 15% safety margin allotted to the fuel, if this margin were not required for another purpose.

6.5 Power System Validation

In this section, the selection of battery component, solar array size and its component will be analyzed to determine whether the requirement is met for the power system. Given the requirement to have 188 W at the end of life (P_{EOL}) for a 3-year mission. We first looked at the minimum required power production by the solar array. With multijunction solar cells, the degradation rate is about 3% per year with conservative assumptions. Assume having the efficiencies of energy storage (η_{Stor}) and distribution (η_{Dist}) of 80% and 90%, respectively. Using the equation given below [22], the minimum required power production at beginning of life (P_{array}) is:

$$P_{array} = P_{EOL} \times \frac{1}{\eta_{Dist}} \frac{BOL}{EOL} \times \left(1 + \frac{1}{\eta_{Stor}} \frac{t_E}{t_o - t_E}\right) = 235\ W$$

where t_o and t_E represent the orbital period and eclipse period. This is the first derived requirement for power system design.

To produce required power, the area of the solar array is computed and drives the second requirement. Assuming that: (1) the solar array efficiency of 28%; (2) the solar irradiance (Φ) is $1366\ W/m^2$; and (3) the solar array always points at the Sun ($\beta = 0°$). The area of solar array could be derived with the equation below:

$$A_{Array} = \frac{P_{array}}{\phi\eta_{array}cos\theta} = 0.614\ \mathrm{m}^2$$

We selected 30 units of UTJ triple junction solar cells. After assembling them together, this gives an area of 0.9 m^2 with a peak power of 240 W, which satisfies both power production and area requirements.

To store the required power during the eclipse period, a carefully sized battery is needed. Assume the number of life cycles of batteries equal to the number of eclipses over 3 years, which is 1467. The Lithium-ion battery is selected due to its high energy density and wide application in satellite battery systems. Looking at the plot [23] below, for a typical Lithium-ion battery on the ground, the theoretical depth of discharge reaches 100% when life cycles are below 2500 cycles. We take it more conservative due to the consideration of solar radiance, and assume the depth of discharge to be equal to 80%.

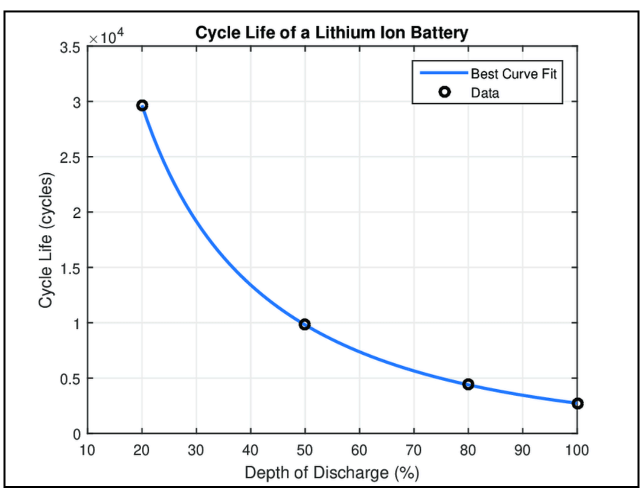

Figure 24. Cycle life of a typical Li-ion battery vs. depth of discharge (DOD)

With the same set of assumptions as previous, the required total battery capacity is 325 Wh.

$$C_{Tot} = \frac{P_{users} t_E}{\eta_{Dist} \times DOD} = 325\ Whr$$

For CNCC, one unit of VES16 8s4p with battery capacity of 512-Whr is selected to meet the power capacity requirement. This gives us a safety margin of about 1.58.

6.6 Delta-V Validation

The overall spacecraft mass, plus the required propellant, ends up being 83.4 kg. Because the overall payload that the Atlas V can carry is 2652 kg, our total mass of 1,668 kg (which already includes several margins) falls well within the constraints put in place by the Atlas V.

The rough dimensions for our spacecraft are in 4 primary parts: the main chassis is 34 cm x 35 cm x 36 cm, the solar cells are 1.94 m x .43 m x 2 cm, the Earth antenna is a 1.1 m parabolic antenna, and the customer antenna is a 0.3 m parabolic antenna. With the antennae and solar panels fully extended, the whole spacecraft takes up a volume of 4.22 m x 3.2 m x 4 m.

For propulsion, our delta V cost was determined by looking at the cost for insertion, stationkeeping, and deorbiting. This led to the following delta V and propellant budget:

Maneuver	Delta V (m/s)	MR	Initial Mass (kg)	Final Mass (kg)	Propellant Budget (kg)	Propellant Budget (kg) 15% margin
Initial insertion	26.44	1.01	68.43	67.81	14.03	16.14
RAAN Separation	29.33	1.01	67.81	67.11	13.41	15.42
Mean Anomaly Separation	38.16	1.01	67.11	66.23	12.71	14.62
Stationkeeping Year 1	80.5	1.03	66.23	64.39	11.83	13.60
Stationkeeping Year 2	80.5	1.03	64.39	62.61	9.99	11.49
Stationkeeping Year 3	80.5	1.03	62.61	60.87	8.21	9.44
Hyperbolic departure	322	1.12	60.87	54.4	6.47	7.44

Table 11. delta V and propellant budget.

The specific impulse was assumed to be 292 s based on the bi-propellant fuel being used.

The initial insertion was calculated based on the errors in insertion produced by deployment from the Atlas V:

Atlas V								
Orbit at Centaur SC Separation				± 3-sigma Errors				
Mission	Apogee km (nmi)	Perigee km (nmi)	Inclination (deg)	Apogee km (nmi)	Perigee km (nmi)	Inclination (deg)	Argument of Perigee (deg)	RAAN (deg)
GTO (Coast ≤ 800 sec)	35,897 (19,383)	195 (105)	25.6	168 (91)	4.6 (2.5)	0.025	0.2	0.22
GTO (Coast ~ 5400 sec)	35,765 (19,312)	4,316 (2,330)	21.7	238 (129)	12.0 (6.5)	0.025	0.37	0.39
Super-Synch	77,268 (41,722)	294.5 (159)	26.4	586 (316)	4.6 (2.5)	0.025	0.32	0.34

Table 12. Atlas V insertion errors

To handle the corrective maneuvers from initial insertion, the maxima of the 3-sigma errors of the Atlas V launch vehicle were selected then the orbital corrective maneuvers were simulated. The maxima of the insertion errors were chosen, because the insertion errors for lunar launches were not publicly available. Furthermore, a 15% propellant margin was added for all major maneuvers in the case of larger insertion errors. Calculating the required burns to correct these errors, we find a required delta-V of 26.44 m/s for each satellite. The next important maneuver involves inserting each satellite into the proper plane and phase within the satellite after initial insertion which requires a delta-V of 67.49 m/s .

The stationkeeping was estimated using the Astrogator targeting algorithm as a part of STK and validated against the results in the Pereira 2019 [5] paper. STK produced required corrective burns that sum to over 80.5 m/s over a year in operation. By estimating this over 3 years, we can get our total corrective burn delta-V and can estimate our required propellant.

Targeting sequences used in the astrogator propagator for delta V calculations can accept input on how the maneuver should be performed. The following scheme for correcting any orbital elements in the simulations was modeled after impulsive feedback control methods [15]. The RAAN and inclination angle corrections use only one impulse for fuel efficiency and occured when passing through either the polar or the equatorial regions using an orbit normal impulsive maneuver. The argument of perigee and the mean anomaly were also corrected together as an orbit element pair, but required two impulsive maneuvers over one orbit and were applied at both the orbit perigee and apogee in the orbit radial direction. The semimajor axis and eccentricity, both products of apogee and perigee insertion errors, were adjusted together through two impulsive maneuvers over one orbit where the thruster fires in the transverse direction.

The final hyperbolic departure, using the moon as a gravity assist and executed at apogee, requires 41.4% of our orbital speed based on the vis viva equation. Using our speed as calculated in STK means we require a delta-V of 322 m/s. To validate these deorbiting strategy, STK was used to simulate a scenario where all satellites in the constellation execute an impulsive maneuver at their apoapsis and their position relative to the moon is recorded over time:

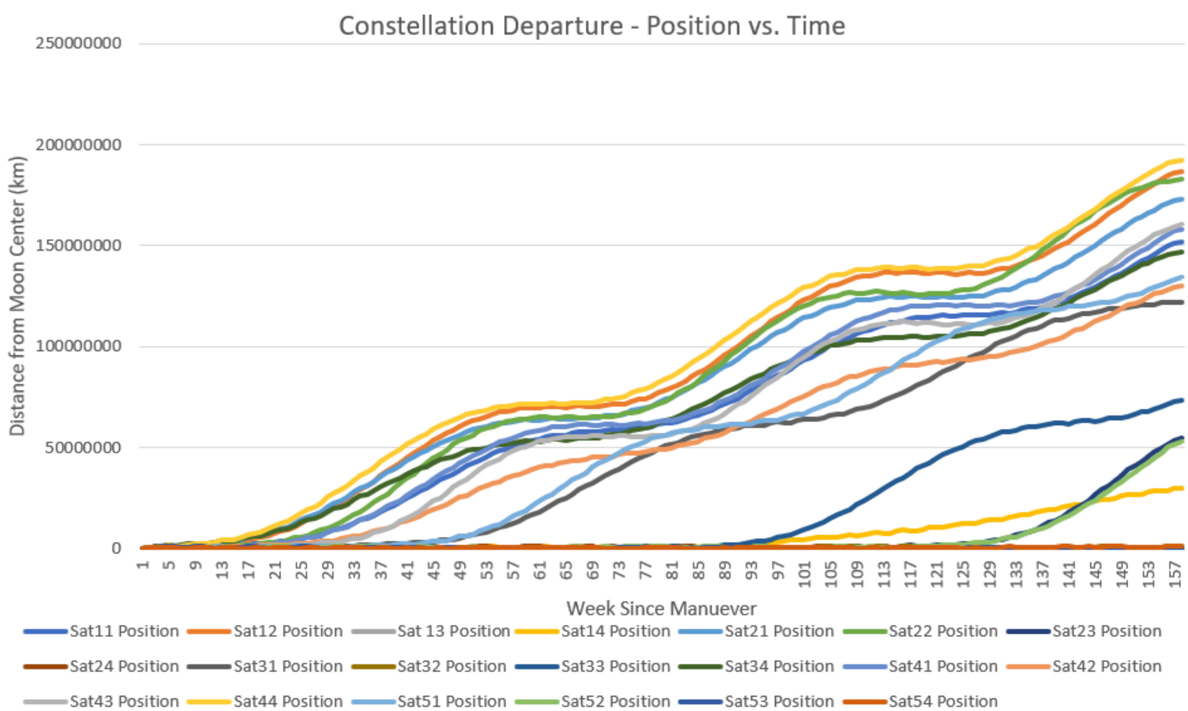

Figure 25 Distance of all CNCC satellites from Moon center after deorbiting maneuver

Here it can be seen that the vast majority of the satellites far exceed the Earth-Moon Distance (more than half exceed 260x the Earth-Moon distance after 3 years). Even the satellites with the smallest distance, Sat54 and Sat13, exceed 3x the Earth-Moon distance and the distance only grows over the 3 years. This validates the deorbiting strategy.

With all of these required burns calculated incrementally through the rocket equation, we end up with a total propellant budget of 17.4 kg per satellite.

6.7 Slew Rate and Disturbance-resistance Validation

In this section, the ADCS is examined to validate the slew rate requirement and maintain the position with interference of disturbance. In the CNCC satellite, three reaction wheels are utilized for regular slew, and momentum storage to prevent frequent momentum dumping, and thrusters for maximum slew and desaturation.

First, the validation of required slew rate is conducted. For a regular slew of 30 deg in 30 second, it needs to produce enough torque along with reaction wheels. With the largest moment of inertia of 9.5 $kg\ m^2$, this yields to:

$$T = 4\theta \frac{I}{t^2} = \frac{4(30\ deg)(\pi/180)(9.5\ kg\ m^2)}{(30\ sec)^2} = 0.022108\ Nm$$

The maximum torque of NewSpace reaction wheels must exceed this number in order to achieve the desired slew rate.

Next, to assess the resistance of reaction wheels to disturbance, several steps are followed to transform the requirement to a comparable measurement. First, an analysis to estimate the worst-case disturbance to the satellite is conducted. The result suggests that solar radiation is the dominating factor over the others, such as aerodynamics, magnetic field, and gravity-induced. The other disturbances are insignificant because there is no atmosphere nor magnetic field around the moon. The gravity-induced disturbance is also negligible due to the fact the satellites are in a high orbit where gravity has much less effect. The solar radiation disturbance is modeled as torque resulting from distance between center of mass (c_g) to center of solar pressure (c_{ps}). Assuming the distance between two centers of 0.3 m, incidence angle (l) of 0 deg, and coefficient of reflectivity (q) of 0.6, for our satellite with cross section of 0.614 m, the equation [4] below finds that:

$$T_{sp} = F(c_{ps} - c_g) = \frac{F_s}{c} A_s(1 + q)cos l(c_{ps} - c_g)$$
$$= \frac{(1367\ W/m^2)(0.614\ m^2)(1+0.6)cos(0)(0.3\ m)}{3\times10^8\ m/s} = 1.3429 \times 10^{-6}\ Nm$$

Note that the worst-case disturbance does not drive the minimum torque requirement of the reaction wheels because it is small compared to torque required for slew. What this leads to is the requirement to have sufficient momentum storage for cyclic torque build-up over an orbit. The minimum required momentum storage [4] is calculated as:

$$h = (T_D)\frac{Orbital\ Period}{4}(0.707)$$

$$= (1.3429 \times 10^{-6}\ Nm)(\frac{64504\ s}{4})(0.707) = 0.015311\ Nms$$

Using the manufacture data, our selection of NewSpace reaction wheels satisfies the requirements with a large margin for both maximum torque and momentum storage.

Actuator Type	Components	Torque Range (Nm)	Momentum Range (Nms)
Reaction Wheel	3x NewSpace NRWA-T2	< 0.1	< 2
Required		0.015311	0.041467

Table 13. Comparison of required and achieved performance for reaction wheels

For the thruster, the required maximum slew rate is not an issue because the force required is relatively small. The constraint here is to make sure the maneuvers for altitude control do not consume very significant propellant and increase the mass budget drastically.

To desaturate the reaction wheels, assuming it performs 1 second impulse, and the frequency for momentum dumping is once per wheel per day. This gives us 3285 pulses over mission lifetime of 3 years and required desaturation force of 0.23037 N.

$$F_{desat} = \frac{h}{Lt} = \frac{0.041467\ Nms}{(0.18m)(1\ sec)} = 0.23037\ N$$

The second requirement is having maximum slew rate of 1 deg/s. Assume thrusters accelerate for 5% of the slew time, and it performs 2 such maneuvers per axis per month, and the result is 0.30705 N with 240 pulses.

$$F_{slew} = \frac{I\theta_a}{L} = \frac{(9.5\ kg\ m^2)(5.8178\times10^{-3} rad/s^2)}{0.18\ m} = 0.30705\ N$$

The total propellant mass[4] is:

$$M_p = \frac{Ft}{I_{sp}g} = \frac{3285\times(0.23037\ N)(1s)+240\times(0.30705\ N)(3s)}{(292\ s)(9.8\ m/s^2)} = 0.31596\ kg$$

per satellite. This is a pretty small number and feasible to finalize this validation.

V. Life Cycle Cost Estimation

The life cycle cost estimation was done in three parts - corresponding to the costs associated with launch, operations, and purchasing the components needed for the system. These costs were added together to get the total system cost.

The most straightforward of these cost estimation techniques was the cost of the launch. As we decided to use the Atlas V, we found that the cost of the rocket is a flat $152 million. This cost allows for the launch of 2652 kilograms of payload into lunar orbit. This value was calculated from the delta-V requirements for launch and orbital insertion and the known component masses and specific impulses of the rocket's engines. While several conservative simplifying assumptions were made, such as the first and second stages operating at their rated specific impulse for sea level, these only assure that the launch system will be able to fulfill its requirements. This result has minimal error, since the launch system we are using has a well-documented price, which was taken from a trusted source [6].

Operations cost estimation was more difficult, but not unreasonably so. First, we estimated that seven engineers would be needed for eight years (based on our team being composed of seven people), and taking approximately five years to develop the satellite, with three years of additional effort needed for the actual operations. We assumed an average salary of 150 thousand dollars per year. Overhead and non-engineering and design jobs would have to be taken into account, necessitating the multiplication of the costs of the engineers by additional factors.

First, a factor was included for the technicians and maintenance personnel required, as well as the support staff for the engineers involved. This was chosen to be six, as it was estimated that these personnel would require roughly half the salary of the engineers, and that it would not be possible for each engineer to oversee more than 12 people directly. Second, a factor for administrative overhead, estimated to be four, was multiplied to this as well. This yielded a fixed cost of $126 million in operations costs for the five-year development period, and another $25.2 million per year of actual operation.

To this was added the cost of using the near-space network for the three-year duration of the mission, which was calculated using the given rate of $557/half-hour [7] to be $9,758,640 per year, discounting leap years. Then, this result was doubled to account for administrative costs and program management, yielding $19,517,280, rounded up to $19.6 million per year. The result of this analysis was an operational budget of 126 million dollars for the five-year development period, as well another 44.8 million dollars per year of mission operation. There were several sources of error in this result, from the lack of data for operations budgets of similar programs making it hard to choose the factors for the technicians and maintenance personnel and administrative costs, to the uncertainty of the salaries of engineers in the future, and the number of engineers that we would need.

Component pricing, in comparison to the first two parts, was extremely difficult to estimate. While most of our components were commercially available, TRL 9, and from reliable sources, most of these sources would not provide pricing information until completion and submission of an invoice. As purchasing the components required was not an option for this analysis, and this would be apparent to anyone we tried to submit an invoice to, this method of cost determination was not in the slightest way viable.

Instead, we opted to use a combination of empirically calculated functions for component cost based on data garnered from previous satellites (adjusted for inflation, of course), and prices on similar components that we could actually find. A number of these formulas were found in Miller [14], and then used to estimate component cost based on mass, power, or proportion of the mass and power of the entire spacecraft used. Additionally, from [14], we also assumed that since 20 units were being produced, economies of scale would also allow the reduction of costs using the method of calculation seen to the right. Note that TFU stands for the theoretical first unit cost. S was approximated to 0.9 since we were producing 10-50 units.

- Calculation:
  - 1) $B = 1 - \frac{\ln((100\%)/S)}{\ln 2}$
  - 2) $L = N^B$
  - 3) Production Cost = TFU x L

  where

  S= Learning Curve slope
  N= Number of units produced
  L= Learning Curve Factor

Of course, this method is extremely vulnerable to unforeseen circumstances, such as technological revolutions (which would bring down the price of the components), or deviations from the average (which could cause an error in either direction). A table of our costs estimates is shown below, showing the cost breakdown of the system.

Notably, as the thermal system we propose to use is currently TRL 5, the price was substantially increased to account for research and development costs, and unexpected issues in production. As these costs also could not be determined to any degree of accuracy, this was simply approximated to an additional factor of four. The integration, assembly and testing costs were assumed to be approximately 24.2% of the market costs of each individual component, to account for the associated risks in assembly. This number was determined by dividing two empirical formulas (Larson, et. al., 796) - for IA&T cost as a function of mass and for spacecraft component cost as a function of mass - which yielded a static ratio.

Portion of System	Subcosts		Total cost
Launch	Atlas V - $152 M		$152 M
Development	$126 M		$126 M
Operations	$44.8 M/yr in operation		$134.4 M
Components	Communications	$16.4 M	$78.9 M
	ADCS	$12.0 M	
	Thermal	$13.4 M	
	Power	$29.0 M	
	Structure	$2.8 M	
	Propulsion	$5.3 M	
Total	N/A		**$491.3 M**

Table 14. Summary of total cost of the mission

VI. Risk Assessment

Risk Matrix						
		Consequence				
		Negligible	Minor	Moderate	Major	Catastrophic
Likelihood	Almost Certain	A, I, J				
	Likely	H				
	Possible			D, E, F		
	Unlikely					K
	Rare		C, G	B		

Table 15. A summary of risks and mitigation measures

A clarification needs to be made here regarding consequences. The scale of consequence is not measured against each individual satellite being able to satisfy their independent subsystem requirements, but rather the ability of the constellation to satisfy mission-level requirements. This is why the failure of a parabolic antenna to deploy can be considered a moderate consequence (A single satellite loses some communication capabilities) on the scale of the whole constellation. The alphabetic code is as follows:

A. High vibrations and G-forces

High vibrations and G-forces are expected during launch and be experienced on release from the Canisterized Satellite Dispenser or during certain propulsive maneuvers (primarily hyperbolic departure). The effects of this risk are potential damage to individual components, destruction of the structure of the satellite, or the dislodging of cables and connectors. Mitigation is performed in design of the structure and through carefully applying techniques that have been used in an innumerable number of previous space missions.

B. Failure of parabolic antenna to deploy

Failure of a parabolic antenna to deploy can occur when deployable mechanisms for the parabolic antenna fail and the structure cannot operate as necessary for communication. This is expected to be relatively rare as many deployable parabolic antennas have been used in recent years, even for very small cubesat satellites [24]. Mitigation is achieved through extensive funding and testing the deployment mechanisms.

C. ADCS Component Failure

The failure of ADCS components, such as reaction wheels and attitude sensors, is when a component fails to perform functionality necessary for a satellite to satisfy its subsystem requirements. The specific effect of this failure depends on the component that fails, but all end up affecting the satellite by influencing the ability of the satellite to accurately point at targets. All component risks are mitigated by the addition of redundant components (1 redundant reaction wheel, an entire ensemble of diverse attitude sensors).

D. High thermal flux from high power components

High thermal flux from high power components means that a lot of heat is passed from a component that is suddenly turned on and consumes a large amount of power. A sudden uptick in heat produced and conducted leads to a high thermal flux that can lead to sudden thermal expansion that can damage components. This can lead to failure of components placed near these high power components (primarily the power amplifier for the communication system). The impact of this risk is mitigated by placing components with redundancy near the power amplifier, slowly ramping power into the component to reduce the sudden thermal expansion, and by adding thermal components such as heat pipes to conduct a lot of the sudden heat flux away and more evenly spread it throughout the spacecraft.

E. **Failure of entry into lunar orbits**

Failure of entry into lunar orbits is when a single satellite in the constellation fails to correct the insertion error from the Atlas V, fails its circularization burn, fails its RAAN corrective maneuver, or fails its mean anomaly phasing. The effect can depend on which of these failures occur, with the worst likely being the failure for mean anomaly phasing which could more readily lead to collisions. This failure can occur if thrusters fail, if propellant leaked, if valves fail to open, or if improper maneuvers are performed due to computer or command errors. This risk is mitigated by slowly performing the sequence with frequent telemetry checks from the ground, this should reduce the risk of the failure being so egregious that it cannot be recovered, and the possibility that one satellite could collide with one another.

F. **Overheating of components**

Overheating of components is when the temperature of a comment exceeds the allowable temperature operating range of the component in question. It can be caused due to too much power consumption by components (outside of expected ranges), failure of radiators to deploy, ignition of propellant/leakage of propellant, or failure of the passive thermal management system due to some structural or design failure. Its effect is to shift components outside of their expected operating environment which could lead to a simple decrease in performance or a complete failure of the component. This risk is mitigated by the thermal management system having redundancy for each component and for the satellite to perform maneuvers that could reduce the amount of incoming heat from the sun to help balance heat within the satellite (for example, orienting the satellite so that the antenna can reflect a large amount of solar radiation, or actuating solar arrays so they are parallel to radiation from the sun).

G. **Failure of solar panel deployment**

Failure of solar panel deployment is when the deployment mechanism for the solar panel fails to extend the solar panel such that it can properly absorb radiation from the sun and perform its photovoltaic function. This can be caused by destruction of deployment mechanisms due to temperature, vibrations, or forces throughout the first two phases of the mission. Its effect is that it limits the amount of power produced by the spacecraft which can affect the ability of the spacecraft to operate normally. This effect is expected to be very rare, as nearly every space mission prior has done solar panel deployment to some extent. Thus, a mitigation strategy beyond using proven mechanisms is unnecessary.

H. Lunar dust from rocket landings

Lunar dust from rocket landings on the lunar surface (or from collisions of spacecraft with the moon) can be kicked into orbit which can affect instrumentation on the satellite or even affect orbit stability. This is almost certain to happen to some extent (perhaps future regulations as the rate of lunar missions increases will decrease the probability of this occurring), but the effects have been demonstrated to be marginal. Especially considering this constellation does not have any particularly sensitive optical equipment, this risk does not warrant much mitigation beyond expecting the effects on orbit stability to consume some of the margin put in place.

I. Radiation (Ionizing dose)

The slow accumulation of ionizing dose from radiation can lead to the failure of space components. This is absolutely certain to happen, and the rates at which the ionizing dose increases with time are relatively well known. The effects of ionizing dose vary per the electrical component being considered, but the general effect is a failure of the component. Mitigation is done by choosing rad-hard electrical components that have a tolerance to an ionizing dose that exceeds the amount of radiation expected over the mission duration. This team was careful to select rad-hard electrical components for this reason, which makes this risk marginal for the current system configuration.

J. Radiation (SEEs)

Certain particles of radiation can be so energetic that they can independently cause macroscale effects in electrical components. This is typically in the form of bit-flips and latch ups in digital computer systems. While this is certain to happen (Usually 100s of times a year), mitigation is incredibly easy as it usually only requires error correction code in software, or in the worst case scenario a reset of the component to reverse the effects.

K. Failure of CSD to deploy satellites

The effect that has the most concern is the failure of the canisterized satellite dispenser to deploy the satellite. The failure of the CSD represents a mission failure. It is considered unlikely due to the simplicity of the CSD and the fact that smaller (but scalable) versions have performed nominally in nearly all previous cubesat missions, but it is not considered rare because a CSD of this size has never been built. This team believes that the analysis of these mechanisms is outside the scope of the class, but that the risk can be mitigated generally by routing a large portion of the mission development towards its development, which is viable considering that the satellites are primarily comprised of COTS which reduces their per unit cost, sparing us some of the budget for the CSD.

VII. Limitations

There are many limitations when it comes to the analysis of our system during this past semester that could be looked into further but may be beyond the scope of this semester-long capstone course. The major parts of our analysis include link budget calculations, STK simulations, GNSS position determination calculations, life cycle cost, mass determination, and ADCS calculations. Each of which have their own set of limitations that should be considered when examining this system.

Through our analysis, the major limitations come from having to make assumptions or not including certain aspects that may be necessary for a high fidelity model. One large group of these limitations was due to our link-budget equation, as assumptions had to be made to simplify the problem to a manageable level.

The first assumption of the link budget equation is that the antennas of the satellite and the near-space network would not be polarized, as classical mechanics can only be reliably used for unpolarized signals - polarized signals must consider different types of interference when being absorbed, which could potentially change the result. Another assumption was that the line-of-sight between the spacecraft and the near-space network could not be obstructed. While we did take into account an average attenuation from the atmosphere and weather effects, any object such as an airplane could potentially shadow the signal due to its opacity, and prevent communication. No extraneous bodies can exist in the Fresnel zone, either. While the Fresnel zone's obstruction is similar in some ways to the obstruction of the line-of-sight, due to the large distances involved quantum effects will cause the waves to form a very skinny ellipsoid instead of a line, and objects near the line of sight can still cause interference that can distort, divert, or attenuate the signal in ways the link-budget equation is ill-suited to accounting for. Additionally, Doppler shifts must be assumed to be negligible for the link-budget equation to operate correctly. While we anticipate slight Doppler shifts, on the order of 10^{-8} times the frequency of the communication, this is not high enough to warrant a more complicated analysis to consider these factors. Antennas were also assumed to have a set, predetermined efficiency, to ease calculation of losses. We also had to assume that the sun was not at any time in the high-gain region of the antenna's view - as the sun produces a vast amount of thermal interference due to its nearly 6000 K temperature, its inclusion in the simulation would likely have increased errors by more than an order of magnitude. Similarly, it was assumed that the blackbody radiation at the signal wavelength encountering the antenna dishes on both our system and the near-space network was negligible compared to the noise temperature of the antenna. Finally, the dishes were assumed to be small relative to the distances at which changes in signal strength become noticeable, so that the signal from each antenna is locally isotropic over the other, and to be significantly farther from each other than the wavelength of the signal. Like many of the previous assumptions, this was done so that the signal could be analyzed classically, instead of requiring the simulation of wave propagation and interference to compute.

The STK simulation also had many limitations in our analysis. We had to decide on our propagator type which all have their trade-offs, the High Precision Orbit Propagator(HPOP) was chosen for the moon in conjunction with Astrogator in STK as it seemed to be the most accurate model for our purposes. HPOP utilizes the Runge-Kutta-Fehlberg method of order 7-8, the Burlirsch-Stoer method, and the Gauss-Jackson method of order 12 for numerical integration. Its orbital propagation is not analytical and the errors from these methods must be negligible. This propagator considers gravity of the parent body, J2, $J2^2$, and J4 effects, solar light pressure and wind, relativistic effects, and atmospheric drag. Astrogator should also consider third body perturbations as this is a major effect when in a high altitude orbit around the moon. The limitations of STK are in the accuracy of these calculations and simulations as well as our limited knowledge of the STK API and lack of documentation when scripting in python. These all affected our ability to create a perfectly accurate model of our constellation.

Another major limitation of our analysis comes from the difficulties of determining the fidelity of our GNSS position determination calculations. When attempting to figure this out, the major issue that arises is our inability to account for multipath losses from the lunar surface to the satellites. These losses are likely going to be very significant in areas of interest on the lunar surface where it may be needed most such as inside of craters and on top of hills and mountains. These will all affect the accuracy of our GNSS system and were not accounted for in our analysis.

The life cycle cost analysis that we performed may be one of the largest limitations for our system as it contains the most assumptions. The major point to cover here is the fact that it is extremely difficult to find the cost for these space rated parts online. In order to get the exact price, most companies and organizations require you to reach out and request a quote which is beyond the scope of where we are at in this project. Therefore, we utilized SMAD to come up with most of our numbers which also has its own limitations. SMAD is getting old at this point and may not be the best estimate for cost validation. However, our analysis provided us with an overall cost that seems reasonable based on the given budget and was given plenty of error margin to cover these limitations and assumptions.

References

1. *Science.gov*, www.science.gov/topicpages/k/ka-band+ground+station.

2. Kegege, Obadiah, et al. "Advances in Ka-band Communication System for CubeSats and SmallSats." 24 June 2016, ntrs.nasa.gov/api/citations/20160010584/downloads/20160010584.pdf.

3. *NASA's Mission Operations and Communications Services*. 2014, deepspace.jpl.nasa.gov/files/6_NASA_MOCS_2014_10_01_14.pdf.

4. Larson, Wiley J., and James R. Wertz. *Space Mission Analysis and Design*. 3rd ed., Microcosm Press, 1999.

5. Pereira, Filipe, and Daniel Selva. *Exploring the Architecture Trade Space of NextGen Global Navigation Satellite Systems*. 2019.

6. "Discover the Value of Launching on ULA's Atlas V." *RocketBuilder*, United Launch Alliance, www.rocketbuilder.com. Accessed 18 Apr. 2022.

7. Near Earth Network and Space Network Cost. NASA's Mission Operations and Communications Services, https://deepspace.jpl.nasa.gov/files/6_NASA_MOCS_2014_10_01_14.pdf

8. CubeStack: CubeSat Space Access,

http://mstl.atl.calpoly.edu/~workshop/archive/2012/Spring/27-Maly-CubeStack.pdf

9. Understanding GPS/GNSS Principles and Applications. Elliott Kaplan and Christopher Hegarty. Artech House. 2017. ISBN-13: 978-1-63081-058-0.

10. Microchip Technology Incorporated. *MAC-SA5X Miniature Atomic Clock.* U.S.A.: Microchip Technology Incorporated, 2021. Web. Accessed 19 Apr 2022.

11. International Lunar Research Station (ILRS) Guide for Partnership,

http://www.cnsa.gov.cn/english/n6465652/n6465653/c6812150/content.html

12. NASA's Lunar Exploration Program Overview,

https://www.nasa.gov/sites/default/files/atoms/files/artemis_plan-20200921.pdf

13. Moore, Terry. "Understanding GPS/GNSS: Principles and Applications, Third Edition Edited by E. D. Kaplan and C. J. Hegarty Artech House, 16 Sussex Street, London, SW1V 4RW, UK. 2017. Xxi; 993pp. Illustrated £155 ISBN 978-1-63081-058-0." *The Aeronautical Journal*, vol. 123, no. 1266, 2019, pp. 1323–1323., doi:10.1017/aer.2019.98.

14. Miller, David. “Space Systems Cost Modelling.” *MIT Open Courseware*, Massachusetts Institute of Technology, 2003, ocw.mit.edu/courses/16-851-satellite-engineering-fall-2003/resources/l15_costmodellec

15. Schaub, H., & Alfriend, K. T. (2001). Impulsive feedback control to establish specific mean orbit elements of spacecraft formations. *Journal of Guidance, Control, and Dynamics*, *24*(4), 739–745. https://doi.org/10.2514/2.4774

16. ”NASA’s Landsat 9 successfully launched aboard Atlas V from Vandenberg.” Mihir Neal & Lee Kanayama. *NASA Spaceflight*. September 27, 2021. https://www.nasaspaceflight.com/2021/09/nasa-landsat-9-launch/

17. ”LEO-MIMO Satellite Systems for High Capacity Transmission.” Daisuke Goto, Hiroki Shibayama, Fumihiro Yamashita, and Takaya Yamazato. Nagoya University. IEEE. 2018. https://ieeexplore.ieee.org/stamp/stamp.jsp?tp=&arnumber=8647694

18. ”MIMO over Satellite: A Review.” Arapoglou et al. IEEE COMMUNICATIONS SURVEYS & TUTORIALS, VOL. 13, NO. 1, FIRST QUARTER 2011. https://ieeexplore.ieee.org/stamp/stamp.jsp?tp=&arnumber=5473886

19. ”Spatial MIMO over Satellite: A Proof of Concept.” Hofmann et al. IEEE ICC 2016 SAC Satellite and Space Communication. https://ieeexplore.ieee.org/stamp/stamp.jsp?tp=&arnumber=7510945

20. "IADC Space Debris Mitigation Guidelines." Inter-Agency Space Debris Coordination Committee. IADC-02-01, Revision 2. March 2020. https://orbitaldebris.jsc.nasa.gov/library/iadc-space-debris-guidelines-revision-2.pdf

21. "Dilution of Precision." Richard Langley. Innovation. GPS World. May 1999. http://gauss.gge.unb.ca/papers.pdf/gpsworld.may99.pdf

22. Chamitoff, Gregory E., and Srinivas R. Vadali, editors. *Human Spaceflight Operations: Lessons Learned from 60 Years in Space*. American Institute of Aeronautics and Astronautics, Inc., 2021, pp. 82-84.

23. Qadrdan, Meysam, et al. *McEvoy's Handbook of Photovoltaics*. 3rd ed., Academic Press, 2018, pp. 915-28.

24. Nanosats Database. "Deployable Parabolic Antenna". January 2022. https://www.nanosats.eu/keyword/deployable-parabolic-antenna